VIBRATION CONTROL OF FGM THICK SHELLS USING HIGHER ORDER SHEAR DEFORMATION THEORY

K. Narendra* and S.C. Pradhan*

Abstract

Analytical solutions of Functionally Graded Material (FGM) shells with embedded magnetostrictive layers are presented in this study. These magnetostrictive layers are used for the vibration suppression of the functionally graded shells. The higher order shear deformation theory (HSDT) is employed to study the vibration suppression characteristics. The exact solution for the FGM shell with simply supported boundary conditions is based on the Navier solution procedure. Negative velocity feedback control is used. The parametric effect of the location of the magnetostrictive layers, material properties, and control parameters on the suppression effect are investigated in detail. Higher order shear deformation theory has significant influence on prediction of vibration response of thick shells. Further, it is found that (i) the shortest vibration suppression time is achieved by placing the actuating layers farthest from the neutral plane (ii) the use of thinner smart material layers leads to better vibration attenuation characteristics, and (iii) the vibration suppression time is longer for a smaller value of the feedback control coefficient.

Keywords*: Functionally graded materials, Higher order, Shear deformation, Vibration, Shell*

Nomenclature

$A_{31}, A_{32}, B_{31}, B_{32}, C_{31}, C_{32}$ = magnetostrictive coefficients

α , β = positive real number

α_1, α_2 = surface matrices

$\varepsilon_1, \varepsilon_2, \varepsilon_6, \gamma_4, \gamma_5$ = total strains

$\varepsilon_1^0, \varepsilon_2^0, \varepsilon_6^0, \gamma_4^0, \gamma_5^0$ = strains from classical shell theory

$\varepsilon_1^1, \varepsilon_2^1, \varepsilon_6^1, \gamma_4^1, \gamma_5^1, \varepsilon_1^2, \varepsilon_2^2, \varepsilon_1^2$ = strains from HSDT

ξ_1, ξ_2, ζ = orthogonal curvilinear co-ordinates

λ = eigen value

λ_0 = arbitrary constant

ϕ_1, ϕ_2 = rotational displacements

ν_1, ν_2 = Poissons ratios of material 1 and material 2

ν_{fgm} = Poissons ratio of FGM material 1 and material 2

ν_m = Poissons ratio of magnetostrictive material

$\rho^{(K)}$ = density of k^{th} layer

ρ_m = density of magnetostrictive material

$\sigma_1, \sigma_2, \sigma_4, \sigma_5, \sigma_6$ = stress components

ω_d = damping frequency

a = length of the shell

b = breadth of the shell

b_c = coil width

$c(t)$ = control gain

dA_1, dA_2 = elementary areas across the thickness of the shell

ds = square of the distance on the middle surface

dS = square of the distance

$e_{31}^k, e_{32}^k, e_{36}^k$ = magnetostrictive material properties of kth layer

*Department of Aerospace Engineering, Indian Institute of Technology Kharagpur, Kharagpur-721 302, West Bengal, India, Email : scp@aero.iitkgp.ernet.in

Manuscript received on 21 Aug 2008; Paper reviewed, revised and accepted on 13 Apr 2009

g_1, g_2 = tangents to ξ_1, ξ_2
h = thickness of the shell
h_m = thickness of magnetostrictive layer
k_c = magnetostrictive coil constant
m, m_1, m_2, n = positive integers
n_c = number of soil turns
nm = number of constituent materials in the FGM
q = uniformly distributed load in the transverse direction
r = position vector on the middle surface
r_c = coil radius
t_n = normalised value of t_s
t_s = suppression time ratio
u_1, u_2, u_3 = displacements at the middle surface
$\bar{u}_1, \bar{u}_2, \bar{u}_3$ = displacements along ξ_1, ξ_2, ζ
z = thickness co-ordinate
$[\,]^0$ = contribution due to classical shell theory
$[\,]^M$ = contribution due to magnetostrictive layer
$A_{ij}, B_{ij}, D_{ij}, E_{ij}, F_{ij}, H_{ij}$ = stiffness coefficients of FGM material
C_1, C_2 = constants which depend on thickness of the shell
E_1, E_2 = Youngs modulus of material 1 and material 2
E_{fgm} = Youngs modulus of FGM material
E_m = Youngs modulus of magnetostrictive material
G_{fgm} = shear modulus of FGM material
H = magnetic field intensity
I = coil current intensity
$I_1, I_2, I_3, I_4, I_5, I_6, I_7$ = moment of inertia
$\bar{I}_i, \bar{J}_i, i = 1, 5$ = terms which depend on inertia terms
L_1, L_2, L_3 = lame coefficients
M_1, M_2, M_6 = moments applied on the edges of the shell
M^M = moments due to the magnetostrictive layer
N = number of layers assumed for computation
N_1, N_2, N_6 = forces applied on the edges of the shell
N^M = forces due to the magnetostrictive layer
P_{-1}, P_1, P_2, P_2 = FGM material constants
P_{fgm} = material property of the FGM material
P_i = material properties of the FGM constituent materials
Q_1, Q_2 = shear forces applied on the edges of the shell
K_1, K_2 = shear forces
$Q_{ij}^{(k)}$ = stiffness coefficients of k^{th} layer
R = position vector of arbitrary point
R_1, R_2 = principal radii of curvature of the middle surface of the shell
R_n = positive real number
S_{ij}, C_{ij}, M_{ij} = coefficients of stiffness, damping and mass matrices
$\bar{S}_{ij}$ = coefficients of solution matrix
T = temperature
V_c = volume fraction of ceramic material
V_{fi} = volume fraction of the constituents of FGM material
V_m = volume fraction of metal material
W_{max} = maximum amplitude in transverse direction
Z_m = transverse location of magnetostrictive layer in the FGM shell

Introduction

A number of materials have been used in sensor/actuator applications. Piezoelectric materials, magnetostrictive materials, shape memory alloys, and electro-rheological fluids have all been integrated with structures to make smart structures. Among these materials piezoelectric, electrostrictive and magnetostrictive mat4erials have the capability to serve as both sensors and actuators. Piezoelectric materials exhibit a linear relationship between the electric field and strains for low field values (up to 100V/mm). This relationship is nonlinear for large fields, and the material exhibits hystersis (Uchino [1]). Further, piezoelectric materials show dielectric aging and hence lack reproducibility of strains, i.e. a drift from zero state of strains is observed under cyclic field applications (Cross and Jang [2]).

Crawley and Luis, [3] demonstrated the feasibility of using piezoelectric actuators for free vibration reduction reduction of a cantilever beam. Baz, et al. [4] investigated vibration control using shape memory alloy and carried out their characterization. Choi, et al. [5] demonstrated the vibration reduction effects of electro rheological fluid actuators in a composite beam. An ideal actuator, for distributed embedded application, should have high en-

ergy density, negligible weight, and point excitation with a wide frequency bandwidth. Terfenol-D, a magnetostrictive material, has the characteristics of being able to produce strains up to 2000 and an energy density as high as $0.0025 Jm^{-3}$ in response to a magnetic field. Goodfriend and Shoop [6] reviewed the material properties of Terfenol-D with regard to its use in vibration isolation. Anjanappa and Bi [7] investigated the feasibility of using embedded magnetostrictive mini actuators for smart structure applications, such as vibration suppression of beams. Bryant et al. [8] presented experimental results of a magnetostrictive Terfonol-D rod used in dual capacity of passive structural support element and an active vibration control actuator. Krishna Murty et al. [9] proposed magnetostrictive actuators that take advantage of ease with which the actuators can be embedded, and the use of remotely excitation capability of magnetostrictive particle as new actuators for smart structures. This work is limited to flexible beam theory.

Friedmann et al. [10] used magnetostrictive material Terfenol-D in high speed helicopter rotors and studied the vibration reduction characteristics. Vibration and shape control of flexible structures is achieved with the help of actuators and a control law. Response of FGM shells are also studied by He, et al. [11], Woo and Meguid [12], Pradhan, et al. [13] and Loy, et al. [14]. Many modern techniques have been developed in recent years to meet the challenge of designing controllers that suit the function under required conditions. There have been a number of studies on vibration control of flexible structures using magnetostrictive materials (Anjanappa and Bi, [7]; Bryant et al. [8]; Krishna Murty et al. [9]; Giurgiutiu et al. [15]; Pradhan et al. [16]; Pradhan [17]). Higher order shear deformation theory is discussed in Reddy [18], Reddy [19] and Reddy [20]. Although there have been important research efforts devoted to characterizing the properties of Terfelon-D material, fundamental information about variation in elasto-magnetic material properties in a thick functionally graded shell is not available.

In the present study vibration control of functionally graded shells are studied using the higher order shear deformation theory. Exact solutions are developed for simply supported doubly curved functionally graded shells with magnetostrictive layers. This closed form solution exists for FGM shells where the coefficients A_{16}, A_{26}, B_{16}, B_{26}, $D_{16,}$ D_{26}, A_{45} are equal to zero. A simple negative velocity feedback control is used to actively control the dynamic response of the structure through a closed loop control. Numerical results of vibration suppression effect for various locations of the magnetostrictive layers, material properties, and control parameters are presented. Influence of HSDT on the thick shells is also investigated.

Theoretical Formulation

Kinematic Description

Figure 1a contains a differential element of a doubly curved shell element with constant curvatures along two coordinate directions (ξ_1, ξ_2), where (ξ_1, ξ_2, ζ) denote the orthogonal curvilinear coordinates such that ξ_1 and ξ_2 curves are the lines of curvature on the middle surface ($\zeta = 0$). Thus, the doubly curved shell panel considered here, the lines of the principal radii of curvature of the middle surface are denoted by R_1 and R_2. The position vector of a point (ξ_1, ξ_2, 0) on the middle surface is denoted by r, and the position of an arbitrary point (ξ_1, ξ_2, ζ) is denoted by **R** (Fig.1b). The square of the distance ds between points (ξ_1, ξ_2, 0) and ($\xi_1 + d\xi_1$, $\xi_2 + d\xi_2$, 0) is determined by

$$(ds)^2 = d\,\mathbf{r} \,.\, d\,\mathbf{r} = \alpha_1^2 (d\,\xi_1)^2 + \alpha_2^2 (d\,\xi_2)^2 \tag{1}$$

in which $d\,\mathbf{r} = \boldsymbol{g}_1\, d\,\xi_1 + \boldsymbol{g}_2\, d\,\xi_2$ the vectors $\mathbf{g}_1$ and $\mathbf{g}_2$ ($\boldsymbol{g}_i = \dfrac{\partial \boldsymbol{r}}{\partial \xi_i}$) are tangent to the ξ_1 and ξ_2 coordinate lines and α_1 and α_2 are the surface metrics

$$\alpha_1^2 = \boldsymbol{g}_1 \cdot \boldsymbol{g}_1, \quad \alpha_2^2 = \boldsymbol{g}_2 \cdot \boldsymbol{g}_2 \tag{2}$$

The square of the distance dS between (ξ_1, ξ_2, ζ) and ($\xi_1 + d\xi_1$, $\xi_2 + d\xi_2$, $\zeta + d\zeta$) is given by

$$(dS)^2 = d\,\mathbf{R} \,.\, d\,\mathbf{R} = L_1^2 (d\,\xi_1)^2 + L_2^2 (d\,\xi_2)^2 + L_3^2 (d\,\zeta)^2 \tag{3}$$

in which $d\mathbf{R} = \left(\dfrac{\partial \mathbf{R}}{\partial \xi_1}\right) d\,\xi_1 + \left(\dfrac{\partial \mathbf{R}}{\partial \xi_2}\right) d\,\xi_2 + \left(\dfrac{\partial \mathbf{R}}{\partial \zeta}\right) d\zeta$ and L_1, L_2 and L_3 are the Lame' coefficients

$$L_1 = \alpha_1 \left(1 + \frac{\zeta}{R_1}\right), \quad L_2 = \alpha_2 \left(1 + \frac{\zeta}{R_2}\right), \quad L_3 = 1 \tag{4}$$

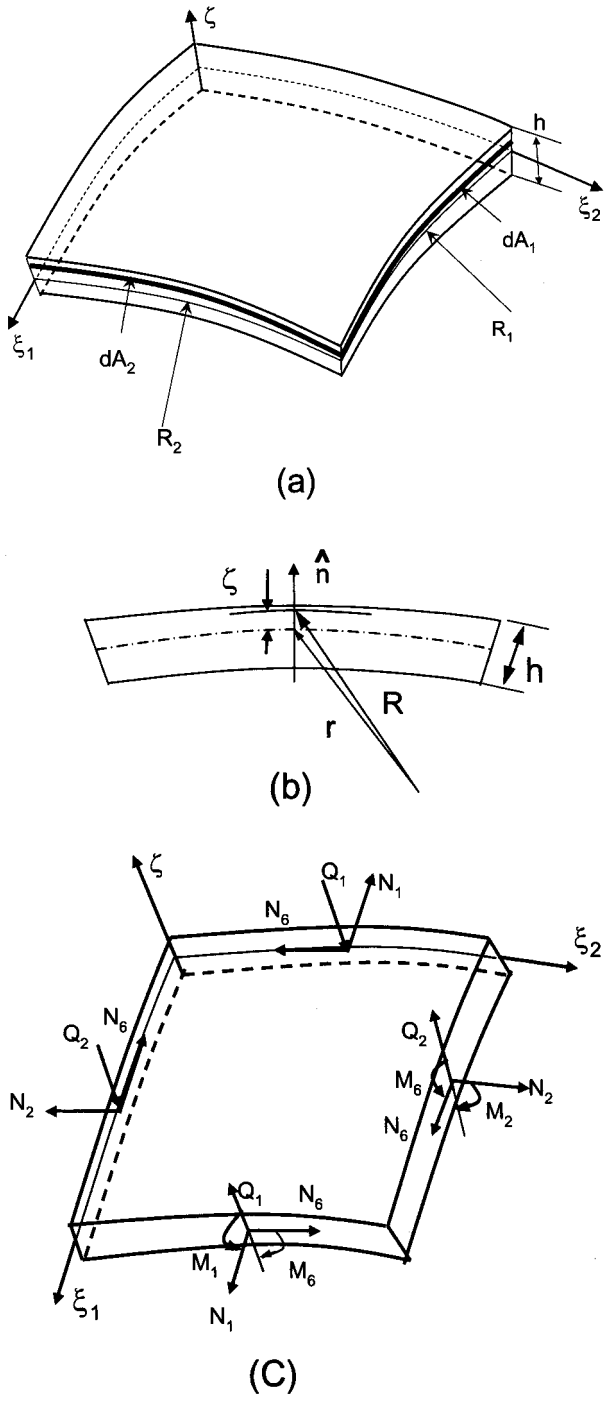

Fig.1 Geometry and Stress Resultants of Doubly Curved Shell

Displacement Field

We assume the following form of the displacement field that his consistent with the assumptions of a thick shell theory as explained in Reddy and Liu [21].

$$\bar{u}_1(\xi_1, \xi_2, \zeta, t) = \frac{L_1}{\alpha_1} u_1(\xi_1, \xi_2, t) + \zeta\phi_1(\xi_1, \xi_2, t) - c_1\zeta^3\left(\phi_1 + \frac{\partial u_3}{\alpha_1 \partial\xi_1}\right)$$

$$\bar{u}_2(\xi_1, \xi_2, \zeta, t) = \frac{L_2}{\alpha_2} u_2(\xi_1, \xi_2, t) + \zeta\phi_2(\xi_1, \xi_2, t) - c_1\zeta^3\left(\phi_2 + \frac{\partial u_3}{\alpha_1 \partial\xi_2}\right)$$

$$\bar{u}_3(\xi_1, \xi_2, \zeta, t) = u_3(\xi_1, \xi_2, t) \tag{5}$$

where

$$\frac{1}{\partial x_i} = \frac{1}{\alpha_i}\frac{1}{\partial \xi_i} (i = 1, 2) \tag{6}$$

$(\bar{u}_1, \bar{u}_2, \bar{u}_3)$ are the displacements of a point (ξ_1, ξ_2, ζ) along the (ξ_1, ξ_2, ζ) coordinates; and $(\bar{u}_1, \bar{u}_2, \bar{u}_3)$ are displacements of a point $(\xi_1, \xi_2, 0)$ on the mid surface of the shell. Substituting equation (5) into strain-displacement relations for the third-order shear deformation theory, one obtains

$$\begin{Bmatrix} \varepsilon_1 \\ \varepsilon_2 \\ \varepsilon_6 \end{Bmatrix} = \begin{Bmatrix} \varepsilon_1^0 \\ \varepsilon_2^0 \\ \varepsilon_6^0 \end{Bmatrix} + \zeta \begin{Bmatrix} \varepsilon_1^1 \\ \varepsilon_2^1 \\ \varepsilon_6^1 \end{Bmatrix} + \zeta^3 \begin{Bmatrix} \varepsilon_1^2 \\ \varepsilon_2^2 \\ \varepsilon_6^2 \end{Bmatrix}$$

$$\begin{Bmatrix} \gamma_4 \\ \gamma_5 \end{Bmatrix} = \begin{Bmatrix} \gamma_4^0 \\ \gamma_5^0 \end{Bmatrix} = \zeta^2 \begin{Bmatrix} \gamma_4^1 \\ \gamma_5^1 \end{Bmatrix} \tag{7}$$

where

$$\begin{Bmatrix} \varepsilon_1^0 \\ \varepsilon_2^0 \\ \varepsilon_6^0 \end{Bmatrix} = \begin{Bmatrix} \dfrac{\partial u_1}{\partial x_1} + \dfrac{1}{R_1} u_3 \\ \dfrac{\partial u_2}{\partial x_2} + \dfrac{1}{R_2} u_3 \\ \dfrac{\partial u_2}{\partial x_1} + \dfrac{\partial u_1}{\partial x_2} \end{Bmatrix}$$

$$\begin{Bmatrix} \varepsilon_1^1 \\ \varepsilon_2^1 \\ \varepsilon_6^1 \end{Bmatrix} = \begin{Bmatrix} \dfrac{\partial \phi_1}{\partial x_1} \\ \dfrac{\partial \phi_2}{\partial x_2} \\ \dfrac{\partial \phi_2}{\partial x_1} + \dfrac{\partial \phi_1}{\partial x_2} \end{Bmatrix}$$

$$\begin{Bmatrix} \varepsilon_1^2 \\ \varepsilon_2^2 \\ \varepsilon_6^2 \end{Bmatrix} = -C_1 \begin{Bmatrix} \dfrac{\partial \phi_1}{\partial x_1} + \dfrac{\partial^2 u_3}{\partial x_1^2} \\ \dfrac{\partial \phi_2}{\partial x_2} + \dfrac{\partial^2 u_3}{\partial x_2^2} \\ \dfrac{\partial \phi_2}{\partial x_1} + \dfrac{\partial \phi_1}{\partial x_2} + 2\dfrac{\partial^2 u_3}{\partial x_1 \partial x_2} \end{Bmatrix}$$

$$\begin{Bmatrix} \gamma_4^0 \\ \gamma_5^0 \end{Bmatrix} = \begin{Bmatrix} \phi_2 + \dfrac{\partial u_3}{\partial x_2} \\ \phi_1 + \dfrac{\partial u_3}{\partial x_1} \end{Bmatrix}$$

$$\begin{Bmatrix} \gamma_4^1 \\ \gamma_5^1 \end{Bmatrix} = -C_2 \begin{Bmatrix} \phi_2 + \dfrac{\partial u_3}{\partial x_2} \\ \phi_1 + \dfrac{\partial u_3}{\partial x_1} \end{Bmatrix} \tag{8}$$

and (ϕ_1, ϕ_2) are rotations of a transverse normal line about the ξ_2 and ξ_1 coordinate axes, respectively.

$$\phi_1 = \frac{\partial u_3}{\partial \xi_1}, \quad \phi_2 = \frac{\partial u_3}{\partial \xi_2} \tag{9}$$

Constants C_1 and C_2 are defined as

$$C_1 = \frac{4}{3h^2}, \; C_2 = 3C_1 \tag{10}$$

Constitutive Relations

Suppose that the shell is composed of N functionally graded layers. The stress-strain relations of the k^{th} layer, whether structural layer or actuating/sensing layer, in the shell coordinate system are given as

$$\begin{Bmatrix} \sigma_1 \\ \sigma_2 \\ \sigma_4 \\ \sigma_5 \\ \sigma_6 \end{Bmatrix}^{(k)} = \begin{bmatrix} Q_{11} & Q_{12} & 0 & 0 & 0 \\ Q_{12} & Q_{22} & 0 & 0 & 0 \\ 0 & 0 & Q_{44} & 0 & 0 \\ 0 & 0 & 0 & Q_{55} & 0 \\ 0 & 0 & 0 & 0 & Q_{66} \end{bmatrix}^{(k)} \begin{Bmatrix} \varepsilon_1 \\ \varepsilon_2 \\ \varepsilon_4 \\ \varepsilon_5 \\ \varepsilon_6 \end{Bmatrix}^{k} - \zeta \begin{Bmatrix} e_{31} \\ e_{32} \\ 0 \\ 0 \\ e_{36} \end{Bmatrix}^{(k)} H \tag{11}$$

where $Q_{ij}^{(k)}$ are the stiffnesses of k^{th} layer.

and

$$Q_{11} = \frac{E_{fgm}}{1-\nu_{fgm}^2}, \quad Q_{12} = \frac{\nu_{fgm} E_{fgm}}{1-\nu_{fgm}^2}, \quad Q_{22} = Q_{11}$$

$$Q_{44} = Q_{55} = Q_{66} = G_{fgm} \tag{12}$$

The superscript k on Q_{ij} as well as on the engineering constants E_{fgm}, ν_{fgm} and so on are omitted for brevity. In equation (11), H denotes the intensity of the magnetic field. H is applied normal to the thickness of the shell. e_{ij} are the magnetostrictive material coefficients.

Feedback Control

A velocity feedback control is used in the present study. In the velocity feedback control, the magnetic field intensity H is expressed in terms of coil current $I(\xi_1, \xi_2, t)$

$$H(\xi_1, \xi_2, t) = k_c I(\xi_1, \xi_2, t) \tag{13}$$

Current I is related to the transverse velocity $\dot{u}_3$ component as

$$I(\xi_1, \xi_2, t) = c(t) \frac{\partial u_3}{\partial t} \tag{14}$$

where k_c is the magnetic coil constant and is related to the number of coil turns n_c coil width b_c, and coil radius r_c

$$k_c = \frac{n_c}{\sqrt{b_c^2 + 4r_c^2}} \tag{15}$$

The parameter *c(t)* is known as the control gain.

Equations of Motion

The governing equations of motion is being derived from the dynamic version of the principle of virtual work for the laminated shell. By integrating the displacement gradients by parts and setting the coefficients of δu_1, δu_2, δu_3, $\delta\phi_1$ and $\delta\phi_2$ to zero separately (the moment terms in the first two equations are omitted) we get

$$\frac{\partial N_1}{\partial x_1} + \frac{\partial N_6}{\partial x_2} = \bar{I}_1 \frac{\partial^2 u_1}{\partial t^2} + \bar{I}_2 \frac{\partial^2 \phi_1}{\partial t^2} - \bar{I}_3 \frac{\partial^2 u_3}{\partial t^2}$$

$$\frac{\partial N_6}{\partial x_1} + \frac{\partial N_2}{\partial x_2} = \bar{J}_1 \frac{\partial^2 u_2}{\partial t^2} + \bar{J}_2 \frac{\partial^2 \phi_2}{\partial t^2} - \bar{J}_3 \frac{\partial^2 u_3}{\partial t^2}$$

$$\frac{\partial Q_1}{\partial x_1} + \frac{\partial Q_2}{\partial x_2} - C_2\left(\frac{\partial K_1}{\partial x_1} + \frac{\partial K_2}{\partial x_2}\right) + C_1\left(\frac{\partial^2 P_1}{\partial x_1^2} + 2\frac{\partial^2 P_6}{\partial x_1 \partial x_2} + \frac{\partial^2 P_2}{\partial x_2^2}\right)$$

$$- \frac{N_1}{R_1} - \frac{N_2}{R_2} + q = \bar{I}_3 \frac{\partial^3 u_1}{\partial x_1 \partial t^2} + \bar{I}_5 \frac{\partial^3 \phi_1}{\partial x_1 \partial t^2} + \bar{J}_3 \frac{\partial^3 u_2}{\partial x_2 \partial t^2}$$

$$+ \bar{J}_5 \frac{\partial^3 \phi_2}{\partial x_2 \partial t^2} + I_1 \frac{\partial^2 u_3}{\partial t^2} - C_1^2 I_7 \left(\frac{\partial^4 u_3}{\partial x_1^2 \partial t^2} + \frac{\partial^4 u_3}{\partial x_2^2 \partial t^2}\right)$$

$$\frac{\partial M_1}{\partial x_1} + \frac{\partial M_6}{\partial x_2} - Q_1 + C_2 K_1 - C_1\left(\frac{\partial P_1}{\partial x_1} + \frac{\partial P_6}{\partial x_2}\right)$$

$$= \bar{I}_2 \frac{\partial^2 u_1}{\partial t^2} + \bar{I}_4 \frac{\partial^2 \phi_1}{\partial t^2} - \bar{I}_5 \frac{\partial^3 u_3}{\partial x_1 \partial t^2}$$

$$\frac{\partial M_6}{\partial x_1} + \frac{\partial M_2}{\partial x_2} - Q_2 + C_2 K_2 - C_1\left(\frac{\partial P_6}{\partial x_1} + \frac{\partial P_2}{\partial x_2}\right)$$

$$= \bar{J}_2 \frac{\partial^2 u_2}{\partial t^2} + \bar{J}_4 \frac{\partial^2 \phi_2}{\partial t^2} - \bar{J}_5 \frac{\partial^3 u_3}{\partial x_2 \partial t^2} \qquad (16)$$

where

$$(N_i, M_i, P_i) = \sum_{k=1}^{N} \int_{\zeta_{k-1}}^{\zeta_k} \sigma_i^{(k)} (1, \zeta, \zeta^3)\, d\zeta \quad (i = 1, 2, 6)$$

$$(Q_1, K_1) = \sum_{k=1}^{N} \int_{\zeta_{k-1}}^{\zeta_k} \sigma_5^{(k)} (1, \zeta^2)\, d\zeta$$

$$(Q_2, K_2) = \sum_{k=1}^{N} \int_{\zeta_{k-1}}^{\zeta_k} \sigma_4^{(k)} (1, \zeta^2)\, d\zeta \qquad (17)$$

$$\bar{I}_1 = I_1 + \frac{2}{R_1} I_2$$

$$\bar{J}_1 = I_1 + \frac{2}{R_2} I_2$$

$$\bar{I}_2 = I_3 + \frac{1}{R_1} I_3 - C_1\left(I_4 + \frac{1}{R_1} I_5\right)$$

$$\bar{J}_2 = I_3 + \frac{1}{R_2} I_3 - C_1\left(I_4 + \frac{1}{R_2} I_5\right)$$

$$I_3 = C_1\left(I_4 + \frac{1}{R_1} I_5\right)$$

$$J_3 = C_1\left(I_4 + \frac{1}{R_2} I_5\right)$$

$$\bar{I}_4 = I_3 - C_1 (2 I_5 - C_1 I_7)$$

$$\bar{J}_4 = \bar{I}_4$$

$$\bar{I}_5 = C_1 (2 I_5 - C_1 I_7)$$

$$\bar{J}_5 = \bar{I}_5 \qquad (18)$$

The inertia terms are defined as

$$(I_1, I_2, I_3, I_4, I_5, I_7) = \sum_{k=1}^{N} \int_{\zeta_{k-1}}^{\zeta_k} \sigma^{(k)} (1, \zeta, \zeta^2, \zeta^3, \zeta^4, \zeta^6)\, d\zeta \qquad (19)$$

where $\rho^{(k)}$ being the density of the k^{th} layer and N is the number of layers in the laminate.

Shell Constitutive Equation

Using equations (7) and (11) in equation (17) we get the following constitutive equations for the actuator embedded shell

$$\begin{Bmatrix} \{N\} \\ \{M\} \\ \{P\} \end{Bmatrix} = \begin{bmatrix} [A] & [B] & [E] \\ [B] & [D] & [F] \\ [E] & [F] & [H] \end{bmatrix} \begin{Bmatrix} \{\varepsilon^0\} \\ \{\varepsilon^1\} \\ \{\varepsilon^2\} \end{Bmatrix} - \begin{Bmatrix} \{N\} \\ \{M\} \\ \{P\} \end{Bmatrix}^M \tag{20}$$

$$\begin{Bmatrix} \{Q\} \\ \{K\} \end{Bmatrix} = \begin{bmatrix} [A] & [D] \\ [D] & [F] \end{bmatrix} \begin{Bmatrix} \gamma^0 \\ \gamma^1 \end{Bmatrix} - \begin{Bmatrix} \{Q\} \\ \{K\} \end{Bmatrix}^M \tag{21}$$

where the shell stiffness coefficients (A_{ij}, B_{ij}, D_{ij}, E_{ij}, F_{ij}, H_{ij} for i,j = 1, 2, 6) are defined by

$$(A_{ij}, B_{ij}, D_{ij}, E_{ij}, F_{ij}, H_{ij}) = \sum_{k=1}^{N} \int_{\zeta k}^{\zeta k+1} \overline{Q}_{ij}^{(k)} \; (1, \zeta, \zeta^2, \zeta^3, \zeta^4, \zeta^6) \, d\zeta \tag{22}$$

and the shell stiffness coefficients (A_{ij}, D_{ij}, F_{ij} for i,j = 4, 5) are defined by

$$(A_{ij}, D_{ij}, F_{ij}) = \sum_{k=1}^{N} \int_{\zeta k}^{\zeta k+1} \overline{Q}_{ij}^{(k)} \; (1, \zeta^2, \zeta^4) \, d\zeta \quad (i, j = 4, 5) \tag{23}$$

The magnetostrictive stress resultants $\{N_i^M\}$, $\{M_i^M\}$ and $\{K_i^M\}$ for (i = 1, 2) are defined as

$$\begin{Bmatrix} \{N_1^M\} \\ \{N_2^M\} \end{Bmatrix} = \sum_{k=m_1,m_2\ldots}^{N} \int_{\zeta k}^{\zeta k+1} \begin{Bmatrix} \{\overline{e}_{31}\} \\ \{\overline{e}_{32}\} \end{Bmatrix} H_\zeta \; d\zeta$$

$$= ck_c \sum_{k=m_1,m_2\ldots}^{N} \int_{\zeta k}^{\zeta k+1} \begin{Bmatrix} \{\overline{e}_{31}\} \\ \{\overline{e}_{32}\} \end{Bmatrix} \frac{\partial u_3}{\partial t} \; d\zeta$$

$$\equiv \begin{Bmatrix} \{A_{31}\} \\ \{A_{32}\} \end{Bmatrix} \frac{\partial u_3}{\partial t} \tag{24}$$

$$\begin{Bmatrix} \{M_1^M\} \\ \{M_2^M\} \end{Bmatrix} = \sum_{k=m_1,m_2\ldots}^{N} \int_{\zeta k}^{\zeta k+1} \begin{Bmatrix} \{\overline{e}_{31}\} \\ \{\overline{e}_{32}\} \end{Bmatrix} \zeta \, H_\zeta \; d\zeta$$

$$= ck_c \sum_{k=m_1,m_2\ldots}^{N} \int_{\zeta k}^{\zeta k+1} \begin{Bmatrix} \{\overline{e}_{31}\} \\ \{\overline{e}_{32}\} \end{Bmatrix} \frac{\partial u_3}{\partial t} \; \zeta \, d\zeta$$

$$\equiv \begin{Bmatrix} \{B_{31}\} \\ \{B_{32}\} \end{Bmatrix} \frac{\partial u_3}{\partial t} \tag{25}$$

$$\begin{Bmatrix} \{K_1^M\} \\ \{K_2^M\} \end{Bmatrix} = \sum_{k=m_1,m_2\ldots}^{N} \int_{\zeta k}^{\zeta k+1} \begin{Bmatrix} \{\overline{e}_{31}\} \\ \{\overline{e}_{32}\} \end{Bmatrix} \zeta^3 \, H_\zeta \; d\zeta$$

$$= ck_c \sum_{k=m_1,m_2\ldots}^{N} \int_{\zeta k}^{\zeta k+1} \begin{Bmatrix} \{\overline{e}_{31}\} \\ \{\overline{e}_{32}\} \end{Bmatrix} \frac{\partial u_3}{\partial t} \; \zeta^3 \, d\zeta$$

$$\equiv \begin{Bmatrix} \{C_{31}\} \\ \{C_{32}\} \end{Bmatrix} \frac{\partial u_3}{\partial t} \tag{26}$$

where

$$A_{ij} = ck_c \sum_{k=m_1,m_2\ldots} \overline{e}_{ij}^{(k)} (\zeta_{k+1} - \zeta_k), \quad i = 3 \; ; \; j = 1, 2$$

$$B_{ij} = \frac{1}{2} ck_c \sum_{k=m_1,m_2\ldots} \overline{e}_{ij}^{(k)} (\zeta_{k+1}^2 - \zeta_k^2), \quad i = 3 \; ; \; j = 1, 2$$

$$C_{ij} = \frac{1}{4} ck_c \sum_{k=m_1,m_2\ldots} \overline{e}_{ij}^{(k)} (\zeta_{k+1}^4 - \zeta_k^4), \quad i = 3 \; ; \; j = 1, 2 \tag{27}$$

and m_1, m_2, ... denote the layer numbers of the magnetostrictive (or any actuating/sensing) layers.

Functionally Graded Material

FGM are basically particles in matrix composite materials, which are made by mixing two or more different materials. Most of the FGM are bending used in high temperature environment and their material properties are temperature dependent. A typical material property P_i can be expressed as a function of the environment temperature *T(K)*

$$P_i = P_0 (P_{-1} T^{-1} + 1 + P_1 T + P_2 T^2 + P_3 T^3)$$

where, P_0, P_{-1}, P_1, P_2 and P_3 are temperature coefficients and are unique to the constituent materials. The material properties P_{fgm} of FGM are controlled by volume fractions V_{fi} and individual material properties P_t of the constituent materials.

$$P_{fgm} = \sum_{i=1}^{n\,m} P_i V_{f\,i} \tag{29}$$

In the present case two different materials are particle mixed to form the FGM material. A schematic of FGM shell with magnetostrictive layers is shown in Figs.2a and 2b. In Fig.2a, it is shown that two layers of magnetostrictive materials are placed symmetrically away from the neutral plane of the FGM shell. A zoomed view of section AA of Fig.2a is shown in Fig.2b. Assuming there are no defects like voids and foreign particles in the FGM material, sum of the volume fractions of all the constituent materials is unity.

$$\sum_{i=1}^{n\,m} V_{f\,i} = 1 \tag{30}$$

For example, metal and ceramic materials ($nm = 2$) are mixed to form the FGM shell. Average volume fraction of the metal and ceramic materials are calculated by simple integration of the distribution over a domain. Different problems of interest have different expressions of volume fractions. For bending problems of plates and shells the volume fractions of metal (V_m) and ceramic (V_c) materials are defined as

$$V_m = \left(\frac{h - 2z}{2h}\right)^{R_n}$$

$$V_c = 1 - V_m \tag{31}$$

Fig.2 (a) Functionally Graded Shell with Embedded Magnetostrictive layers with an (b) Exploded Section View

where z is the thickness co-ordinate ($-h/2 \le z = \le h/2$) and h represents the shell thickness. R_n is the power law exponent ($0 \le R_n \le \infty$). Here volume fraction of the metal material (V_m) varies from 100 percent to 0 percent as z varies from *-h/2* to *h/2*. Similarly volume fraction of the ceramic material (V_c) varies from 0 percent to 100 percent as z varies from *-h/2* to *h/2*. for various R_n values the average volume fractions of metal (V_m) and ceramic (V_c) materials are depicted in Figs.3a and 3b, respectively. The Young's modulus and Poissons ratio of a FGM shell made up of two different materials are expressed as

$$E_{fgm} = (E_2 - E_1) \left(\frac{2z + h}{2h}\right)^{R_n} + E_1 \tag{32}$$

$$\nu_{fgm} = (\nu_2 - \nu_1) \left(\frac{2z + h}{2h}\right)^{R_n} + \nu_1 \tag{33}$$

E_1 E_2 and E_{fgm} are the Youngs moduli of the constituent materials and the FGM material, respectively. ν_1 ν_2 and ν_{fgm} are the Poissons ratios of the constituent materials and the FGM material, respectively. From these equations (32, 33), it is interesting to note that at $z = -h/2$, FGM material properties are same as those of material 1. While at $z = h/2$, FGM material properties are same as those of material 2. Thus, the FGM material properties very smoothly across thickness, from material 1 at the inner surface to material 2 at the outer surface.

Fig.3 Volume Fractions of Metal and Ceramic Materials in the FGM Shell

Two different FGM materials are considered for the present study viz. FGM1 and FGM2. FGM1 consists of Stainless Steel and Nickel materials (Fig.2a). FGM2 consists of Nickel and Aluminum Oxide materials. Material properties of Stainless Steel, Nickel materials and Aluminum Oxide are listed in Table-1. In the present work, we have used the room temperature to calculate the material properties of the FGM shells.

Analytical Solution

The equations of motion (16) can be expressed in terms of displacements (u_1, u_2, u_3, ϕ_1, ϕ_2) by substituting for the force and moment resultants from Eqs.(20, 21). For homogeneous shells, the equations of motion (16) take the following form

$$A_{11}\left(\frac{\partial^2 u_1}{\partial x_1^2}+\frac{1}{R_1}\frac{\partial u_3}{\partial x_1}\right)+A_{12}\left(\frac{\partial^2 u_2}{\partial x_1 \partial x_2}+\frac{1}{R_2}\frac{\partial u_3}{\partial x_1}\right)+A_{16}\left(\frac{\partial^2 u_2}{\partial x_1^2}+\frac{\partial^2 u_1}{\partial x_1 \partial x_2}\right)$$

$$+B_{11}\frac{\partial^2 \phi_1}{\partial x_1^2}+B_{12}\frac{\partial^2 \phi_2}{\partial x_1 \partial x_2}+B_{16}\left(\frac{\partial^2 \phi_2}{\partial x_1^2}+\frac{\partial^2 \phi_1}{\partial x_1 \partial x_2}\right)-C_1 E_{11}\left(\frac{\partial^2 \phi_1}{\partial x_1^2}+\frac{\partial^3 u_3}{\partial x_1^3}\right)$$

$$-C_1 E_{12}\left(\frac{\partial^2 \phi_2}{\partial x_1 \partial x_2}+\frac{\partial^3 u_3}{\partial x_1 \partial x_2^2}\right)-C_1 E_{16}\left(\frac{\partial^2 \phi_2}{\partial x_1^2}+\frac{\partial^2 \phi_1}{\partial x_1 \partial x_2}+2\frac{\partial^3 u_3}{\partial x_1^2 \partial x_2}\right)$$

$$-A_{31}\frac{\partial^2 u_3}{\partial x_1 \partial t}+A_{16}\left(\frac{\partial^2 u_1}{\partial x_1 \partial x_2}+\frac{1}{R_1}\frac{\partial u_3}{\partial x_2}\right)+A_{26}\left(\frac{\partial^2 u_2}{\partial x_2^2}+\frac{1}{R_2}\frac{\partial u_3}{\partial x_2}\right)$$

Table-1 : Material Properties of FGM Constituent Materials

	Stainless Steel		Nickel		Aluminium Oxide	
Density (kg m^{-3}	7900		8909		3970	
Coefficient	E (Nm^{-2})	ν	E (Nm^{-2})	ν	E (Nm^{-2})	ν
P_0	201.04E09	0.3262	244.27E09	0.2882	349.55E09	0.260
P_{-1}	0	0	0	0	0	0
P_1	3.079E-04	-2.002E-04	-1.371E-03	1.133E-04	-3.853E-04	0
P_2	-6.534E-07	3.797E-07	1.214E-06	0	4.027E-07	0
P_3	0	0	-3.681E-10	0	-1.673E-10	0

$$+A_{66}\left(\frac{\partial^2 u_2}{\partial x_1 \partial x_2}+\frac{\partial^2 u_1}{\partial x_2^2}\right)+B_{16}\frac{\partial^2 \phi_1}{\partial x_1 \partial x_2}+B_{26}\frac{\partial^2 \phi_2}{\partial x_2^2}+B_{66}\left(\frac{\partial^2 \phi_2}{\partial x_1 \partial x_2}+\frac{\partial^2 \phi_1}{\partial x_2^2}\right)$$

$$-C_1 E_{16}\left(\frac{\partial^2 \phi_1}{\partial x_1 \partial x_2}+\frac{\partial^2 u_3}{\partial x_1^2 \partial x_2}\right)-C_1 E_{26}\left(\frac{\partial^2 \phi_2}{\partial x_2^2}+\frac{\partial^3 u_3}{\partial x_2^3}\right)$$

$$-C_1 E_{66}\left(\frac{\partial^2 \phi_2}{\partial x_1 \partial x_2}+\frac{\partial^2 \phi_1}{\partial x_2^2}+2\frac{\partial^3 u_3}{\partial x_1 \partial x_2^2}\right)-\bar{I}_1\frac{\partial^2 u_1}{\partial t^2}-\bar{I}_2\frac{\partial^2 \phi_1}{\partial t^2}+\bar{I}_3\frac{\partial^2 u_3}{\partial x_1 \partial t^2}=0 \quad (34)$$

$$A_{16}\left(\frac{\partial^2 u_1}{\partial x_1^2}+\frac{1}{R_1}\frac{\partial u_3}{\partial x_1}\right)+A_{26}\left(\frac{\partial^2 u_2}{\partial x_1 \partial x_2}+\frac{1}{R_2}\frac{\partial u_3}{\partial x_1}\right)+A_{66}\left(\frac{\partial^2 u_2}{\partial x_1^2}+\frac{\partial^2 u_1}{\partial x_1 \partial x_2}\right)$$

$$+B_{16}\frac{\partial^2 \phi_1}{\partial x_1^2}+B_{26}\frac{\partial^2 \phi_2}{\partial x_1 \partial x_2}+B_{66}\left(\frac{\partial^2 \phi_2}{\partial x_1^2}+\frac{\partial^2 \phi_1}{\partial x_1 \partial x_2}\right)-C_1 E_{16}\left(\frac{\partial^2 \phi_1}{\partial x_1^2}+\frac{\partial^3 u_3}{\partial x_1^3}\right)$$

$$-C_1 E_{26}\left(\frac{\partial^2 \phi_2}{\partial x_1 \partial x_2}+\frac{\partial^3 u_3}{\partial x_1 \partial x_2^2}\right)-C_1 E_{66}\left(\frac{\partial^2 \phi_2}{\partial x_1^2}+\frac{\partial^2 \phi_1}{\partial x_1 \partial x_2}+2\frac{\partial^3 u_3}{\partial x_1^2 \partial x_2}\right)$$

$$+A_{12}\left(\frac{\partial^2 u_1}{\partial x_1 \partial x_2}+\frac{1}{R_1}\frac{\partial u_3}{\partial x_2}\right)+A_{22}\left(\frac{\partial^2 u_2}{\partial x_2^2}+\frac{1}{R_2}\frac{\partial u_3}{\partial x_2}\right)$$

$$+A_{26}\left(\frac{\partial^2 u_2}{\partial x_1 \partial x_2}+\frac{\partial^2 u_1}{\partial x_2^2}\right)+B_{12}\frac{\partial^2 \phi_1}{\partial x_1 \partial x_2}+B_{22}\frac{\partial^2 \phi_2}{\partial x_2^2}+B_{26}\left(\frac{\partial^2 \phi_2}{\partial x_1 \partial x_2}+\frac{\partial^2 \phi_1}{\partial x_2^2}\right)$$

$$-C_1 E_{12}\left(\frac{\partial^2 \phi_1}{\partial x_1 \partial x_2}+\frac{\partial^2 u_3}{\partial x_1^2 \partial x_2}\right)-C_1 E_{22}\left(\frac{\partial^2 \phi_2}{\partial x_2^2}+\frac{\partial^3 u_3}{\partial x_2^3}\right)$$

$$-C_1 E_{26}\left(\frac{\partial^2 \phi_2}{\partial x_1 \partial x_2}+\frac{\partial^2 \phi_1}{\partial x_2^2}+2\frac{\partial^3 u_3}{\partial x_1 \partial x_2^2}\right)-A_{32}\frac{\partial^2 u_3}{\partial x_2 \partial t}$$

$$-\bar{J}_1\frac{\partial^2 u_2}{\partial t^2}-\bar{J}_2\frac{\partial^2 \phi_2}{\partial t^2}+\bar{J}_3\frac{\partial^3 u_3}{\partial x_2 \partial t^2}=0 \quad (35)$$

$$A_{45}\left(\frac{\partial \phi_2}{\partial x_1}+\frac{\partial^2 u_3}{\partial x_1 \partial x_2}\right)+A_{55}\left(\frac{\partial \phi_1}{\partial x_1}+\frac{\partial^2 u_3}{\partial^2 x_1}\right)-C_2 D_{45}\left(\frac{\partial \phi_2}{\partial x_1}+\frac{\partial^2 u_3}{\partial x_1 \partial x_2}\right)$$

$$-C_2 D_{55}\left(\frac{\partial \phi_1}{\partial x_1}+\frac{\partial^2 u_3}{\partial^2 x_1}\right)+A_{44}\left(\frac{\partial \phi_2}{\partial x_2}+\frac{\partial^2 u_3}{\partial^2 x_2}\right)+A_{45}\left(\frac{\partial \phi_1}{\partial x_2}+\frac{\partial^2 u_3}{\partial x_1 \partial x_2}\right)$$

$$-C_2 D_{44}\left(\frac{\partial \phi_2}{\partial x_2}+\frac{\partial^2 u_3}{\partial^2 x_2}\right)-C_2 D_{45}\left(\frac{\partial \phi_1}{\partial x_2}+\frac{\partial^2 u_3}{\partial x_1 \partial x_2}\right)$$

$$-C_2 D_{45}\left(\frac{\partial \phi_2}{\partial x_1}+\frac{\partial^2 u_3}{\partial x_1 \partial x_2}\right)-C_2 D_{55}\left(\frac{\partial \phi_1}{\partial x_1}+\frac{\partial^2 u_3}{\partial^2 x_1}\right)$$

$$+C_2^2 F_{45}\left(\frac{\partial \phi_2}{\partial x_1}+\frac{\partial^2 u_3}{\partial x_1 \partial x_2}\right)-C_2^2 F_{55}\left(\frac{\partial \phi_1}{\partial x_1}+\frac{\partial^2 u_3}{\partial^2 x_1}\right)$$

$$-C_2 D_{44}\left(\frac{\partial \phi_2}{\partial x_2}+\frac{\partial^2 u_3}{\partial x_2^2}\right)-C_2 D_{45}\left(\frac{\partial \phi_1}{\partial x_2}+\frac{\partial^2 u_3}{\partial x_1 \partial x_2}\right)$$

$$-C_2^2 F_{44}\left(\frac{\partial \phi_2}{\partial x_2}+\frac{\partial^2 u_3}{\partial x_2^2}\right)-C_2^2 F_{45}\left(\frac{\partial \phi_1}{\partial x_2}+\frac{\partial^2 u_3}{\partial x_1 \partial x_2}\right)$$

$$+C_1 E_{11}\left(\frac{\partial^3 u_1}{\partial x_1^3}+\frac{1}{R_1}\frac{\partial^2 u_3}{\partial x_1^2}\right)+C_1 E_{12}\left(\frac{\partial^3 u_2}{\partial x_1^2 \partial x_2}+\frac{1}{R_2}\frac{\partial^2 u_3}{\partial x_1^2}\right)$$

$$+C_1 E_{16}\left(\frac{\partial^3 u_2}{\partial x_1^3}+\frac{\partial^3 u_1}{\partial x_1^2 \partial x_2}\right)+C_1 F_{11}\frac{\partial^3 \phi_1}{\partial x_1^3}$$

$$-C_1^2 H_{11}\left(\frac{\partial^3 \phi_1}{\partial x_1^3}+\frac{\partial^4 u_3}{\partial x_1^4}\right)-C_1^2 H_{12}\left(\frac{\partial^3 \phi_2}{\partial x_1^2 \partial x_2}+\frac{\partial^4 u_3}{\partial x_1^2 \partial x_2^2}\right)$$

$$-C_1^2 H_{16}\left(\frac{\partial^3 \phi_2}{\partial x_1^3}+\frac{\partial^3 \phi_1}{\partial x_1^2 \partial x_2}+2\frac{\partial^4 u_3}{\partial x_1^3 \partial x_2}\right)-C_1 C_{31}\frac{\partial^3 u_3}{\partial x_1^2 \partial t}$$

$$+2C_1 E_{16}\left(\frac{\partial^3 u_1}{\partial x_1^2 \partial x_2}+\frac{1}{R_1}\frac{\partial^2 u_3}{\partial x_1 \partial x_2}\right)+2C_1 E_{26}\left(\frac{\partial^3 u_3}{\partial x_1 \partial x_2^2}+\frac{1}{R_2}\frac{\partial^2 u_3}{\partial x_1 \partial x_2}\right)$$

$$+2C_1E_{66}\left(\frac{\partial^3 u_2}{\partial x_1^2\partial x_2}+\frac{\partial^3 u_1}{\partial x_1\partial x_2^2}\right)+2C_1F_{16}\frac{\partial^3\phi_1}{\partial x_1^2\partial x_2}+2C_1F_{26}\frac{\partial^3\phi_2}{\partial x_1\partial x_2^2}$$

$$+2C_1F_{66}\left(\frac{\partial^3\phi_2}{\partial x_1^2\partial x_2}+\frac{\partial^3\phi_1}{\partial x_1\partial x_2^2}\right)-2C_1^2H_{16}\left(\frac{\partial^3\phi_1}{\partial x_1^2\partial x_2}+\frac{\partial^4 u_3}{\partial x_1^3\partial x_2}\right)$$

$$-2C_1^2H_{26}\left(\frac{\partial^3\phi_2}{\partial x_1\partial x_2^2}+\frac{\partial^4 u_3}{\partial x_1\partial x_2^3}\right)-2C_1^2H_{66}\left(\frac{\partial^3\phi_2}{\partial x_1^2\partial x_2}+\frac{\partial^3\phi_1}{\partial x_1\partial x_2^2}+2\frac{\partial^4 u_3}{\partial x_1^2\partial x_2^2}\right)$$

$$+C_1E_{12}\left(\frac{\partial^3 u_1}{\partial x_1\partial x_2^2}+\frac{1}{R_1}\frac{\partial^2 u_3}{\partial x_2^2}\right)+C_1E_{22}\left(\frac{\partial^3 u_2}{\partial x_2^3}+\frac{1}{R_2}\frac{\partial^2 u_3}{\partial x_2^2}\right)$$

$$+C_1E_{26}\left(\frac{\partial^3 u_2}{\partial x_1\partial x_2^2}+\frac{\partial^3 u_1}{\partial x_2^3}\right)+C_1F_{12}\frac{\partial^3\phi_1}{\partial x_1\partial x_2^2}+C_1F_{22}\frac{\partial^3\phi_2}{\partial x_2^3}$$

$$+C_1F_{26}\left(\frac{\partial^3\phi_2}{\partial x_1\partial x_2^2}+\frac{\partial^3\phi_1}{\partial x_2^3}\right)-C_1^2H_{12}\left(\frac{\partial^3\phi_1}{\partial x_1\partial x_2^2}+\frac{\partial^4 u_3}{\partial x_1^2\partial x_2^2}\right)$$

$$-C_1^2H_{22}\left(\frac{\partial^3\phi_2}{\partial x_2^3}+\frac{\partial^4 u_3}{\partial x_2^4}\right)-C_1^2H_{26}\left(\frac{\partial^3\phi_2}{\partial x_1\partial x_2^2}+\frac{\partial^3\phi_1}{\partial x_2^3}+2\frac{\partial^4 u_3}{\partial x_1\partial x_2^3}\right)$$

$$-C_1C_{32}\frac{\partial^3 u_3}{\partial x_2^2\partial t}-\frac{1}{R_1}A_{11}\left(\frac{\partial u_1}{\partial x_1}+\frac{u_3}{R_1}\right)-\frac{1}{R_1}A_{12}\left(\frac{\partial u_2}{\partial x_2}+\frac{u_3}{R_2}\right)$$

$$-\frac{1}{R_1}A_{16}\left(\frac{\partial u_2}{\partial x_2}+\frac{\partial u_1}{\partial x_2}\right)-\frac{1}{R_1}B_{11}\frac{\partial\phi_1}{\partial x_1}-\frac{1}{R_1}B_{12}\frac{\partial\phi_2}{\partial x_2}-\frac{1}{R_1}B_{16}\left(\frac{\partial\phi_2}{\partial x_1}+\frac{\partial\phi_1}{\partial x_2}\right)$$

$$+C_1\frac{1}{R_1}E_{11}\left(\frac{\partial\phi_1}{\partial x_1}+\frac{\partial^2 u_3}{\partial x_1^2}\right)+C_1\frac{1}{R_1}E_{12}\left(\frac{\partial\phi_2}{\partial x_2}+\frac{\partial^2 u_3}{\partial x_2^2}\right)$$

$$+C_1\frac{1}{R_1}E_{16}\left(\frac{\partial\phi_2}{\partial x_1}+\frac{\partial\phi_1}{\partial x_2}+2\frac{\partial^2 u_3}{\partial x_1\partial x_2}\right)+\frac{1}{R_1}A_{31}\frac{\partial u_3}{\partial t}$$

$$-\frac{1}{R_2}A_{12}\left(\frac{\partial u_1}{\partial x_1}+\frac{u_3}{R_1}\right)-\frac{1}{R_2}A_{22}\left(\frac{\partial u_2}{\partial x_2}+\frac{u_3}{R_2}\right)-\frac{1}{R_2}A_{26}\left(\frac{\partial u_2}{\partial x_1}+\frac{\partial u_1}{\partial x_2}\right)$$

$$-\frac{1}{R_2}B_{12}\frac{\partial\phi_1}{\partial x_1}-\frac{1}{R_1}B_{22}\frac{\partial\phi_2}{\partial x_2}-\frac{1}{R_2}B_{26}\left(\frac{\partial\phi_2}{\partial x_1}+\frac{\partial\phi_1}{\partial x_2}\right)$$

$$+C_1\frac{1}{R_2}E_{12}\left(\frac{\partial\phi_1}{\partial x_1}+\frac{\partial^2 u_3}{\partial x_1^2}\right)+C_1\frac{1}{R_2}E_{22}\left(\frac{\partial\phi_2}{\partial x_2}+\frac{\partial^2 u_3}{\partial x_2^2}\right)$$

$$+C_1\frac{1}{R_2}E_{26}\left(\frac{\partial\phi_2}{\partial x_1}+\frac{\partial\phi_1}{\partial x_2}+2\frac{\partial^2 u_3}{\partial x_1\partial x_2}\right)+\frac{1}{R_2}A_{32}\frac{\partial u_3}{\partial t}+q$$

$$-\bar{I}_1\frac{\partial^2 u_3}{\partial t^2}+\bar{I}_3\frac{\partial^3 u_1}{\partial x_1\partial t^2}-\bar{I}_5\frac{\partial^3\phi_1}{\partial x_1\partial t^2}-\bar{J}_3\frac{\partial^3 u_2}{\partial x_2\partial t^2}-\bar{J}_5\frac{\partial^3\phi_2}{\partial x_2\partial t^2}$$

$$+C_1^2I_7\left(\frac{\partial^4 u_3}{\partial x_1^2\partial t^2}+\frac{\partial^4 u_3}{\partial x_2^2\partial t^2}\right)=0 \qquad (36)$$

$$B_{11}\left(\frac{\partial^2 u_1}{\partial x_1^2}+\frac{1}{R_1}\frac{\partial u_3}{\partial x_1}\right)+B_{12}\left(\frac{\partial^2 u_2}{\partial x_1\partial x_2}+\frac{1}{R_2}\frac{\partial u_3}{\partial x_1}\right)+B_{16}\left(\frac{\partial^2 u_2}{\partial x_1^2}+\frac{\partial^2 u_1}{\partial x_1\partial x_2}\right)$$

$$+D_{11}\frac{\partial^2\phi_1}{\partial x_1^2}+D_{12}\frac{\partial^2\phi_2}{\partial x_1\partial x_2}+D_{16}\left(\frac{\partial^2\phi_2}{\partial x_1^2}+\frac{\partial^2\phi_1}{\partial x_1\partial x_2}\right)-C_1F_{11}\left(\frac{\partial^2\phi_1}{\partial x_1^2}+\frac{\partial^3 u_3}{\partial x_1^3}\right)$$

$$-C_1F_{12}\left(\frac{\partial^2\phi_2}{\partial x_1\partial x_2}+\frac{\partial^3 u_3}{\partial x_1\partial x_2^2}\right)-C_1F_{16}\left(\frac{\partial^2\phi_2}{\partial x_1^2}+\frac{\partial^2\phi_1}{\partial x_1\partial x_2}+2\frac{\partial^3 u_3}{\partial x_1^2\partial x_2}\right)$$

$$-B_{31}\frac{\partial^2 u_3}{\partial x_1\partial t}+B_{16}\left(\frac{\partial^2 u_1}{\partial x_1\partial x_2}+\frac{1}{R_1}\frac{\partial u_3}{\partial x_2}\right)+B_{26}\left(\frac{\partial^2 u_2}{\partial x_2^2}+\frac{1}{R_2}\frac{\partial u_3}{\partial x_2}\right)$$

$$+B_{66}\left(\frac{\partial^2 u_2}{\partial x_1\partial x_2}+\frac{\partial^2 u_1}{\partial x_2^2}\right)+D_{16}\frac{\partial^2\phi_1}{\partial x_1\partial x_2}+D_{26}\frac{\partial^2\phi_2}{\partial x_2^2}$$

$$+D_{66}\left(\frac{\partial^2\phi_2}{\partial x_1\partial x_2}+\frac{\partial^2\phi_1}{\partial x_2^2}\right)-C_1F_{16}\left(\frac{\partial^2\phi_1}{\partial x_1\partial x_2}+\frac{\partial^2 u_3}{\partial x_1^2\partial x_2}\right)$$

$$-C_1F_{26}\left(\frac{\partial^2\phi_2}{\partial x_2^2}+\frac{\partial^2 u_3}{\partial x_2^3}\right)-C_1F_{66}\left(\frac{\partial^2\phi_2}{\partial x_1\partial x_2}+\frac{\partial^2\phi_1}{\partial x_2^2}+2\frac{\partial^3 u_3}{\partial x_1\partial x_2^2}\right)$$

$$- A_{45}\left(\phi_2 + \frac{\partial u_3}{\partial x_2}\right) - A_{55}\left(\phi_1 + \frac{\partial u_3}{\partial x_1}\right) + C_2 D_{45}\left(\phi_2 + \frac{\partial u_3}{\partial x_2}\right)$$

$$+ C_2 D_{55}\left(\phi_1 + \frac{\partial u_3}{\partial x_1}\right) + C_2 D_{45}\left(\phi_2 + \frac{\partial u_3}{\partial x_2}\right)$$

$$+ C_2 D_{55}\left(\phi_1 + \frac{\partial u_3}{\partial x_1}\right) + C_2^2 F_{45}\left(\phi_2 + \frac{\partial u_3}{\partial x_2}\right)$$

$$- C_2^2 F_{55}\left(\phi_1 + \frac{\partial u_3}{\partial x_1}\right) - C_1 E_{11}\left(\frac{\partial^2 u_1}{\partial x_1^2} + \frac{1}{R_1}\frac{\partial u_3}{\partial x_1}\right)$$

$$- C_1 E_{12}\left(\frac{\partial^2 u_2}{\partial x_1 \partial x_2} + \frac{1}{R_2}\frac{\partial u_3}{\partial x_1}\right) - C_1 E_{16}\left(\frac{\partial^2 u_2}{\partial x_1^2} + \frac{\partial^2 u_1}{\partial x_1 \partial x_2}\right)$$

$$- C_1 F_{11}\frac{\partial^2 \phi_1}{\partial x_1^2} - C_1 F_{12}\frac{\partial^2 \phi_2}{\partial x_1 \partial x_2}$$

$$- C_1 F_{16}\left(\frac{\partial^2 \phi_2}{\partial x_1^2} + \frac{\partial^2 \phi_1}{\partial x_1 \partial x_2}\right) + C_1^2 H_{11}\left(\frac{\partial^2 \phi_1}{\partial x_1^2} + \frac{\partial^3 u_3}{\partial x_1^3}\right)$$

$$+ C_1^2 H_{12}\left(\frac{\partial^2 \phi_2}{\partial x_1 \partial x_2} + \frac{\partial^3 u_3}{\partial x_1 \partial x_2^2}\right) + C_1^2 H_{16}\left(\frac{\partial^2 \phi_2}{\partial x_1^2} + \frac{\partial^2 \phi_1}{\partial x_1 \partial x_2} + 2\frac{\partial^3 u_3}{\partial x_1^2 \partial x_2}\right)$$

$$+ C_1 C_{31}\frac{\partial^2 u_3}{\partial x_1 \partial t} - C_1 E_{16}\left(\frac{\partial^2 u_1}{\partial x_1 \partial x_2} + \frac{1}{R_1}\frac{\partial u_3}{\partial x_2}\right)$$

$$- C_1 E_{26}\left(\frac{\partial^2 u_2}{\partial x_2^2} + \frac{1}{R_2}\frac{\partial u_3}{\partial x_2}\right) - C_1 E_{66}\left(\frac{\partial^2 u_2}{\partial x_1 \partial x_2} + \frac{\partial^2 u_1}{\partial x_2^2}\right)$$

$$- C_1 F_{16}\frac{\partial^2 \phi_1}{\partial x_1 \partial x_2} - C_1 F_{26}\frac{\partial^2 \phi_2}{\partial x_2^2} - C_1 F_{66}\left(\frac{\partial^2 \phi_2}{\partial x_1 \partial x_2} + \frac{\partial^2 \phi_1}{\partial x_2^2}\right)$$

$$+ C_1^2 H_{16}\left(\frac{\partial^2 \phi_1}{\partial x_1 \partial x_2} + \frac{\partial^3 u_3}{\partial x_1^2 \partial x_2}\right) + C_1^2 H_{26}\left(\frac{\partial^2 \phi_2}{\partial x_2^2} + \frac{\partial^3 u_3}{\partial x_2^3}\right)$$

$$+ C_1^2 H_{66}\left(\frac{\partial^2 \phi_2}{\partial x_1 \partial x_2} + \frac{\partial^2 \phi_1}{\partial x_2^2} + 2\frac{\partial^3 u_3}{\partial x_1 \partial x_2^2}\right) - \bar{I}_2\frac{\partial^2 u_1}{\partial t^2} - \bar{I}_4\frac{\partial^2 \phi_1}{\partial t^2}$$

$$+ \bar{I}_5\frac{\partial^2 u_3}{\partial x_1 \partial t^2} = 0 \qquad (37)$$

$$B_{16}\left(\frac{\partial^2 u_1}{\partial x_1^2} + \frac{1}{R_1}\frac{\partial u_3}{\partial x_1}\right) + B_{26}\left(\frac{\partial^2 u_2}{\partial x_1 \partial x_2} + \frac{1}{R_2}\frac{\partial u_3}{\partial x_1}\right) + B_{66}\left(\frac{\partial^2 u_2}{\partial x_1^2} + \frac{\partial^2 u_1}{\partial x_1 \partial x_2}\right)$$

$$+ D_{16}\frac{\partial^2 \phi_1}{\partial x_1^2} + D_{26}\frac{\partial^2 \phi_2}{\partial x_1 \partial x_2} + D_{66}\left(\frac{\partial^2 \phi_2}{\partial x_1^2} + \frac{\partial^2 \phi_1}{\partial x_1 \partial x_2}\right) - C_1 F_{16}\left(\frac{\partial^2 \phi_1}{\partial x_1^2} + \frac{\partial^3 u_3}{\partial x_1^3}\right)$$

$$- C_1 F_{26}\left(\frac{\partial^2 \phi_2}{\partial x_1 \partial x_2} + \frac{\partial^3 u_3}{\partial x_1 \partial x_2^2}\right) - C_1 F_{66}\left(\frac{\partial^2 \phi_2}{\partial x_1^2} + \frac{\partial^2 \phi_1}{\partial x_1 \partial x_2} + 2\frac{\partial^3 u_3}{\partial x_1^2 \partial x_2}\right)$$

$$+ B_{12}\left(\frac{\partial^2 u_1}{\partial x_1 \partial x_2} + \frac{1}{R_1}\frac{\partial u_3}{\partial x_2}\right) + B_{22}\left(\frac{\partial^2 u_2}{\partial x_2^2} + \frac{1}{R_2}\frac{\partial u_3}{\partial x_2}\right)$$

$$+ B_{26}\left(\frac{\partial^2 u_2}{\partial x_1 \partial x_2} + \frac{\partial^2 u_1}{\partial x_2^2}\right) + D_{12}\frac{\partial^2 \phi_1}{\partial x_1 \partial x_2} + D_{22}\frac{\partial^2 \phi_2}{\partial x_2^2}$$

$$+ D_{26}\left(\frac{\partial^2 \phi_2}{\partial x_1 \partial x_2} + \frac{\partial^2 \phi_1}{\partial x_2^2}\right) - C_1 F_{12}\left(\frac{\partial^2 \phi_1}{\partial x_1 \partial x_2} + \frac{\partial^2 u_3}{\partial x_1^2 \partial x_2}\right)$$

$$- C_1 F_{22}\left(\frac{\partial^2 \phi_2}{\partial x_2^2} + \frac{\partial^2 u_3}{\partial x_2^3}\right) - C_1 F_{26}\left(\frac{\partial^2 \phi_2}{\partial x_1 \partial x_2} + \frac{\partial^2 \phi_1}{\partial x_2^2} + 2\frac{\partial^3 u_3}{\partial x_1 \partial x_2^2}\right)$$

$$- B_{32}\frac{\partial^2 u_3}{\partial x_2 \partial t} - A_{44}\left(\phi_2 + \frac{\partial u_3}{\partial x_2}\right) - A_{45}\left(\phi_1 + \frac{\partial u_3}{\partial x_1}\right) + C_2 D_{44}\left(\phi_2 + \frac{\partial u_3}{\partial x_2}\right)$$

$$+ C_2 D_{45}\left(\phi_1 + \frac{\partial u_3}{\partial x_1}\right) + C_2 D_{44}\left(\phi_2 + \frac{\partial u_3}{\partial x_2}\right)$$

$$+ C_2 D_{45}\left(\phi_1 + \frac{\partial u_3}{\partial x_1}\right) - C_2^2 F_{44}\left(\phi_2 + \frac{\partial u_3}{\partial x_2}\right)$$

$$
\begin{aligned}
&- C_2^2 F_{45}\left(\phi_1 + \frac{\partial u_3}{\partial x_1}\right) - C_1 E_{16}\left(\frac{\partial^2 u_1}{\partial x_1^2} + \frac{1}{R_1}\frac{\partial u_3}{\partial x_1}\right) \\
&- C_1 E_{26}\left(\frac{\partial^2 u_2}{\partial x_1 \partial x_2} + \frac{1}{R_2}\frac{\partial u_3}{\partial x_1}\right) - C_1 E_{66}\left(\frac{\partial^2 u_2}{\partial x_1^2} + \frac{\partial^2 u_1}{\partial x_1 \partial x_2}\right) \\
&- C_1 F_{16}\frac{\partial^2 \phi_1}{\partial x_1^2} - C_1 F_{26}\frac{\partial^2 \phi_2}{\partial x_1 \partial x_2} \\
&- C_1 F_{66}\left(\frac{\partial^2 \phi_2}{\partial x_1^2} + \frac{\partial^2 \phi_1}{\partial x_1 \partial x_2}\right) + C_1^2 H_{16}\left(\frac{\partial^2 \phi_1}{\partial x_1^2} + \frac{\partial^3 u_3}{\partial x_1^3}\right) \\
&+ C_1^2 H_{26}\left(\frac{\partial^2 \phi_2}{\partial x_1 \partial x_2} + \frac{\partial^3 u_3}{\partial x_1 \partial x_2^2}\right) + C_1^2 H_{66}\left(\frac{\partial^2 \phi_2}{\partial x_1^2} + \frac{\partial^2 \phi_1}{\partial x_1 \partial x_2} + 2\frac{\partial^3 u_3}{\partial x_1^2 \partial x_2}\right) \\
&- C_1 E_{12}\left(\frac{\partial^2 u_1}{\partial x_1 \partial x_2} + \frac{1}{R_1}\frac{\partial u_3}{\partial x_2}\right) - C_1 E_{22}\left(\frac{\partial^2 u_2}{\partial x_2^2} + \frac{1}{R_2}\frac{\partial u_3}{\partial x_2}\right) \\
&- C_1 E_{26}\left(\frac{\partial^2 u_2}{\partial x_1 \partial x_2} + \frac{\partial^2 u_1}{\partial x_2^2}\right) - C_1 F_{12}\frac{\partial^2 \phi_1}{\partial x_1 \partial x_2} - C_1 F_{22}\frac{\partial^2 \phi_2}{\partial x_2^2} \\
&- C_1 F_{26}\left(\frac{\partial^2 \phi_2}{\partial x_1 \partial x_2} + \frac{\partial^2 \phi_1}{\partial x_2^2}\right) + C_1^2 H_{12}\left(\frac{\partial^2 \phi_1}{\partial x_1 \partial x_2} + \frac{\partial^3 u_3}{\partial x_1^2 \partial x_2}\right) \\
&+ C_1^2 H_{22}\left(\frac{\partial^2 \phi_2}{\partial x_2^2} + \frac{\partial^3 u_3}{\partial x_2^3}\right) + C_1^2 H_{26}\left(\frac{\partial^2 \phi_2}{\partial x_1 \partial x_2} + \frac{\partial^2 \phi_1}{\partial x_2^2} + 2\frac{\partial^3 u_3}{\partial x_1 \partial x_2^2}\right) \\
&+ C_1 C_{32}\frac{\partial^2 u_3}{\partial x_2 \partial t} - \bar{J}_2\frac{\partial^2 u_2}{\partial t^2} - \bar{J}_4\frac{\partial^2 \phi_2}{\partial t^2} + \bar{J}_5\frac{\partial^3 u_3}{\partial x_2 \partial t^2} = 0
\end{aligned}
\tag{38}
$$

Exact solution for the partial differential equations (16) on arbitrary domains and for general boundary conditions is not possible. However, for simply supported shells whose projection in the x_1, x_2-plane is a rectangle and for a lamination scheme of antisymmetric cross-ply or symmetric cross-ply type equations (16) are solved exactly. The Navier solution exists if the following stiffnesses are zero (Reddy 1984a).

$$
\begin{aligned}
&A_{i6} = B_{i6} = D_{i6} = E_{i6} = F_{i6} = H_{i6} = 0 \quad (i = 1, 2) \quad \text{and} \\
&A_{45} = D_{45} = F_{45} = 0
\end{aligned}
\tag{39}
$$

The simply-supported boundary conditions for the higher order shear deformation theory (HSDT) are assumed to be

$$
\begin{aligned}
&u_1(x_1, 0, t) = 0, \quad u_1(x_1, b, t) = 0, \quad u_2(0, x_2, t) = 0, \quad u_2(a, x_2, t) = 0 \\
&u_3(x_1, 0, t) = 0, \quad u_3(x_2, b, t) = 0, \quad u_3(0, x_2, t) = 0, \quad u_3(a, x_2, t) = 0 \\
&N_1(0, x_2, t) = 0, \quad N_1(a, x_2, t) = 0, \quad N_2(x_1, 0, t) = 0, \quad N_2(x_1, b, t) = 0 \\
&M_1(0, x_2, t) = 0, \quad M_1(a, x_2, t) = 0, \quad M_2(x_1, 0, t) = 0, \quad M_2(x_1, b, t) = 0 \\
&P_1(0, x_2, t) = 0, \quad P_1(a, x_2, t) = 0, \quad P_2(x_1, 0, t) = 0, \quad P_2(x_1, b, t) = 0 \\
&\phi_1(x_1, 0, t) = 0, \quad \phi_1(x_1, b, t) = 0, \quad \phi_2(0, x_2, t) = 0, \quad \phi_2(a, x_2, t) = 0
\end{aligned}
\tag{40}
$$

where a and b denote the lengths along x_1 and x_2 directions, respectively. The boundary conditions in equation (40) are satisfied by the following expansions (Reddy 1997).

$$
\begin{aligned}
u_1(x_1, x_2, t) &= \sum_{n=1}^{\infty}\sum_{m=1}^{\infty} U_{mn}(t)\cos\alpha x_1 \sin\beta x_2 \\
u_2(x_1, x_2, t) &= \sum_{n=1}^{\infty}\sum_{m=1}^{\infty} V_{mn}(t)\sin\alpha x_1 \sin\beta x_2 \\
u_3(x_1, x_2, t) &= \sum_{n=1}^{\infty}\sum_{m=1}^{\infty} W_{mn}(t)\sin\alpha x_1 \sin\beta x_2 \\
\phi_1(x_1, x_2, t) &= \sum_{n=1}^{\infty}\sum_{m=1}^{\infty} X_{mn}(t)\cos\alpha x_1 \sin\beta x_2 \\
\phi_2(x_1, x_2, t) &= \sum_{n=1}^{\infty}\sum_{m=1}^{\infty} Y_{mn}(t)\sin\alpha x_1 \cos\beta x_2
\end{aligned}
\tag{41}
$$

Substituting equation (41) into equation (38) we obtain

$$\begin{bmatrix} S_{11} & S_{12} & S_{13} & S_{14} & S_{15} \\ S_{21} & S_{22} & S_{23} & S_{24} & S_{25} \\ S_{31} & S_{32} & S_{33} & S_{34} & S_{35} \\ S_{41} & S_{42} & S_{43} & S_{44} & S_{45} \\ S_{51} & S_{52} & S_{53} & S_{54} & S_{55} \end{bmatrix} \begin{Bmatrix} U_{m\,n} \\ V_{m\,n} \\ W_{m\,n} \\ X_{m\,n} \\ Y_{m\,n} \end{Bmatrix}$$

$$+ \begin{bmatrix} 0 & 0 & C_{13} & 0 & 0 \\ 0 & 0 & C_{23} & 0 & 0 \\ 0 & 0 & C_{33} & 0 & 0 \\ 0 & 0 & C_{43} & 0 & 0 \\ 0 & 0 & C_{53} & 0 & 0 \end{bmatrix} \begin{Bmatrix} \dot{U}_{m\,n} \\ \dot{V}_{m\,n} \\ \dot{W}_{m\,n} \\ \dot{X}_{m\,n} \\ \dot{Y}_{m\,n} \end{Bmatrix}$$

$$+ \begin{bmatrix} M_{11} & 0 & M_{13} & M_{14} & 0 \\ 0 & M_{22} & M_{23} & 0 & M_{25} \\ M_{31} & M_{32} & M_{33} & M_{34} & M_{35} \\ M_{41} & 0 & M_{43} & M_{44} & 0 \\ 0 & M_{52} & M_{53} & 0 & M_{55} \end{bmatrix} \begin{Bmatrix} \ddot{U}_{m\,n} \\ \ddot{V}_{m\,n} \\ \ddot{W}_{m\,n} \\ \ddot{X}_{m\,n} \\ \ddot{Y}_{m\,n} \end{Bmatrix} = \begin{Bmatrix} 0 \\ 0 \\ Q_{m\,n} \\ 0 \\ 0 \end{Bmatrix} \tag{42}$$

Where S_{ij}, C_{ij} and M_{ij} (i, j = 1,2, ... 5) are written in equations (48-50) in the appendix. For vibration control, we assume $q = 0$ and seek solution of the ordinary differential equations in equation (42) in the form

$$U_{m\,n}(t) = U_0 e^{\lambda t},\ V_{m\,n}(t) = V_0 e^{\lambda t},\ W_{m\,n}(t) = W_0 e^{\lambda t},$$

$$X_{m\,n}(t) = X_0 e^{\lambda t},\ Y_{m\,n}(t) = Y_0 e^{\lambda t} \tag{43}$$

Substituting equation (43) into equation (42), for a non-trivial solution we obtain the result

$$\begin{bmatrix} \bar{S}_{11} & \bar{S}_{12} & \bar{S}_{13} & \bar{S}_{14} & \bar{S}_{15} \\ \bar{S}_{21} & \bar{S}_{22} & \bar{S}_{23} & \bar{S}_{24} & \bar{S}_{25} \\ \bar{S}_{31} & \bar{S}_{32} & \bar{S}_{33} & \bar{S}_{34} & \bar{S}_{35} \\ \bar{S}_{41} & \bar{S}_{42} & \bar{S}_{43} & \bar{S}_{44} & \bar{S}_{45} \\ \bar{S}_{51} & \bar{S}_{52} & \bar{S}_{53} & \bar{S}_{54} & \bar{S}_{55} \end{bmatrix} 0 \tag{44}$$

where

$$\bar{S}_{ij} = S_{ij} + \lambda C_{ij} + \lambda^2 M_{ij} \text{ (for } i, j = 1, 2, 3, 4, 5) \tag{45}$$

This equation gives five sets of eigenvalues. The lowest one corresponds to the transverse motion. The eigenvalue can be written as $\lambda = -\alpha + i\,\omega_d$, so that the damped motion is given by

$$u_3(x_1, x_2, t) = \frac{1}{\omega_d} e^{-\alpha t} \sin \omega_d t \sin \frac{n \pi x_1}{a} \sin \frac{n \pi x_2}{b} \tag{46}$$

In arriving at the last solution, the following boundary conditions are used:

$$u_1(x_1, x_2, 0) = 0,\ \dot{u}_1(x_1, x_2, 0) = 0,\ u_2(x_1, x_2, 0) = 0,$$

$$\dot{u}_2(x_1, x_2, 0) = 0,\ u_3(x_1, x_2, 0) = 0,\ \dot{u}_3(x_1, x_2, 0) = 1,$$

$$\phi_1(x_1, x_2, 0) = 0,\ \dot{\phi}_1(x_1, x_2, 0) = 0,\ \phi_2(x_1, x_2, 0) = 0,$$

$$\dot{\phi}_2(x_1, x_2, 0) = 0 \tag{47}$$

Results and Discussions

In the present work a theoretical analysis of a functionally graded material (FGM) shell, consisting of layers of magnetostrictive material. The magnetostrictive material is assumed to impart vibration control through a velocity dependent feedback law that controls the current to the magnetic coils energizing the magnetostrictive material. Higher order shear deformation theory (HSDT) is used in the derivation. Numerical simulation results are presented. Effect of various parameters on the vibration suppression time is studied. These parameters are (a) location of magnetostrictive layer from the neutral plane (b) thickness of magnetostrictive layer (c) higher modes of vibration (d) material properties of magnetostrictive material and (e) material properties of FGM material. Further influence of

Table-2a : Various Coefficients of FGM1 (Stainless Steel-Nickel) Shell									
Z_m m	F_{11} Nm^3 (10^1)	H_{11} Nm^5 (10^{-3})	D_{11} Nm (10^6)	F_{12} Nm^3 (10^1)	H_{12} Nm^5 (10^{-3})	D_{12} Nm (10^5)	F_{22} Nm^3 (10^1)	H_{22} Nm^5 (10^{-3})	D_{22} Nm (10^6)
0.0095	0.624	0.375	0.124	0.178	0.103	0.366	0.624	0.375	0.124
0.0085	0.752	0.534	0.132	0.222	0.157	0.393	0.752	0.534	0.132
0.0075	0.843	0.622	0.139	0.253	0.187	0.417	0.843	0.622	0.139
0.0065	0.904	0.668	0.145	0.274	0.203	0.438	0.904	0.668	0.145
0.0055	0.942	0.689	0.150	0.287	0.210	0.456	0.942	0.689	0.150
0.0045	0.964	0.698	0.155	0.294	0.213	0.471	0.964	0.698	0.155
0.0035	0.976	0.701	0.158	0.298	0.214	0.483	0.976	0.701	0.158
0.0025	0.981	0.702	0.161	0.300	0.215	0.492	0.981	0.702	0.161
0.0015	0.983	0.702	0.163	0.301	0.215	0.498	0.983	0.702	0.163
0.0005	0.983	0.702	0.164	0.301	0.215	0.501	0.983	0.702	0.164

Table-2b : Various Coefficients of FGM1 (Stainless Steel-Nickel) Shell								
Z_m m	F_{66} Nm^3 (10^1)	H_{66} Nm^5 (10^{-3})	D_{66} Nm (10^5)	F_{44} Nm^3 (10^1)	D_{44} Nm^5 (10^5)	A_{44} Nm^{-1} (10^{10})	F_{55} Nm^3 (10^1)	D_{55} Nm (10^5)
0095	0.223	0.136	0.438	0.223	0.438	0.156	0.223	0.438
0085	0.265	0.188	0.464	0.265	0.464	0.156	0.265	0.464
0075	0.295	0.217	0.487	0.295	0.487	0.156	0.295	0.487
0065	0.315	0.232	0.507	0.315	0.507	0.156	0.315	0.507
0055	0.328	0.239	0.525	0.328	0.525	0.156	0.328	0.525
0045	0.335	0.242	0.539	0.335	0.539	0.156	0.335	0.539
0035	0.339	0.243	0.551	0.339	0.551	0.156	0.339	0.551
0025	0.340	0.244	0.559	0.340	0.559	0.156	0.340	0.559
0015	0.341	0.244	0.565	0.341	0.565	0.156	0.341	0.565
0005	0.341	0.244	0.568	0.341	0.568	0.156	0.341	0.568

higher order shear deformation shell theory on vibration response of thick shells are investigated.

The FGM shell is considered to be of 1m x 1m dimension. Two different types of FGM shells (FGM1 and FGM2) are considered for the present study. FGM1 is made up of Stainless Steel and Nickel. FGM2 is made up of Nickel and Aluminum Oxide. For most of the present work FGM1 is employed. IN the present work if it is not mentioned FGM2 means it is FGM1 shell. The material properties of constituent materials, Stainless Steel, Nickel and Aluminum Oxide of the FGM shells are listed in Table-1. Two layers of magnetostrictive materials are placed symmetrically away from the neutral plane of the FGM shell. These layers are shown in Fig.2a. A zoomed view of section AA of Fig.2a is shown in Fig.2b. Magnetostrictive material properties are considered to be

$$E_m = 26.5 \text{ GPa},\ \nu_m = 0.0,\ \rho_m = 9250\ \text{kg} - \text{m}^{-3},\ c\,(t)\, r_c = 10^4 \tag{48}$$

Table-2c : Various Coefficients of FGM1 (Stainless Steel-Nickel) Shell

Z_m m	C_1 m^{-2} (10^4)	C_2 m^{-2} (10^5)	I_1 kgm^{-2} (10^2)	I_3 kg (10^{-2})	I_5 kgm^2 (10^{-6})	I_7 kgm^4 (10^{10})	$-B_{31}$ (10^2)	$-C_{31}$ (10^{-2})
0095	0.333	0.100	0.849	0.288	0.175	0.126	0.841	0.761
0085	0.333	0.100	0.849	0.288	0.175	0.126	0.752	0.545
0075	0.333	0.100	0.849	0.285	0.171	0.126	0.664	0.375
0065	0.333	0.100	0.849	0.284	0.170	0.121	0.575	0.244
0055	0.333	0.100	0.849	0.283	0.169	0.120	0.487	0.148
0045	0.333	0.100	0.849	0.282	0.168	0.120	0.398	0.082
0035	0.333	0.100	0.849	0.281	0.168	0.120	0.310	0.039
0025	0.333	0.100	0.849	0.281	0.168	0.120	0.221	0.014
0015	0.333	0.100	0.849	0.280	0.168	0.120	0.133	0.003
0005	0.333	0.100	0.849	0.280	0.168	0.120	0.044	0.000

Table-3a : Various Coefficients of FGM2 (Nickel-Aluminum Oxide) Shell

Z_m m	F_{11} Nm^3 (10^1)	H_{11} Nm^5 (10^{-3})	D_{11} Nm (10^6)	F_{12} Nm^3 (10^1)	H_{12} Nm^5 (10^{-3})	D_{12} Nm (10^5)	F_{22} Nm^3 (10^1)	H_{22} Nm^5 (10^{-3})	D_{22} Nm (10^6)
0.0095	0.801	0.478	0.161	0.207	0.119	0.426	0.801	0.478	0.161
0.0085	0.974	0.691	0.171	0.258	0.182	0.457	0.974	0.691	0.171
0.0075	1.095	0.809	0.181	0.294	0.218	0.485	1.095	0.809	0.181
0.0065	1.177	0.871	0.189	0.318	0.236	0.509	1.177	0.871	0.189
0.0055	1.228	0.899	0.196	0.333	0.244	0.530	1.228	0.899	0.196
0.0045	1.258	0.911	0.202	0.342	0.248	0.547	1.258	0.911	0.202
0.0035	1.274	0.915	0.207	0.347	0.249	0.561	1.274	0.915	0.207
0.0025	1.281	0.916	0.210	0.349	0.249	0.572	1.281	0.916	0.210
0.0015	1.283	0.916	0.212	0.349	0.249	0.579	1.283	0.916	0.212
0.0005	1.283	0.916	0.214	0.349	0.249	0.583	1.283	0.916	0.214

The numerical values of various materials and structural constants based on different locations of magnetostrictive layers and FGM material properties are listed in Tables-2 and 3. In this study, the vibration suppression time (t_s) is defined as the time required to reduce the uncontrolled vibration amplitude to one-tenth of its initial amplitude. In the present numerical simulations the suppression time, thickness of the magnetostrictive layer are denoted by t_s and hm, respectively. Z_m represents the distance between the location of the magnetostrictive layer and the neutral plane.

Effect of Magnetostrictive Layer Location

Effect of location of magnetostrictive layers on the vibration suppression is studied. Fig.2a and 2b show the location of magnetostrictive layers in the FGM shells. Transverse deflection versus time for Z_m of 3.5mm, 5.5mm 7.5mm and 9.5mm are plotted in Figs.4a, 4b, 4c and 4d respectively. For Z_m equals to 9.5mm, Fig.4d shows shortest suppression time (t_s) of 0.22 Seconds and for Z_m equals to 3.5mm, Fig.4a shows longest suppression time (t_s) of 0.59 Seconds. From Figs. 4a-4d, shortest

Table-3b : Various Coefficients of FGM2 (Nickel-Aluminum Oxide) Shell								
Z_m m	F_{66} Nm^3 (10^1)	H_{66} Nm^5 (10^{-3})	D_{66} Nm (10^5)	F_{44} Nm^3 (10^1)	D_{44} Nm^5 (10^5)	A_{44} Nm^{-1} (10^{10})	F_{55} Nm^3 (10^1)	D_{55} Nm (10^5)
0.0095	0.297	0.179	0.591	0.297	0.591	0.212	0.297	0.591
0.0085	0.358	0.254	0.628	0.358	0.628	0.212	0.358	0.628
0.0075	0.401	0.296	0.661	0.401	0.661	0.212	0.401	0.661
0.0065	0.429	0.317	0.690	0.429	0.690	0.212	0.429	0.690
0.0055	0.447	0.327	0.715	0.447	0.715	0.212	0.447	0.715
0.0045	0.458	0.332	0.736	0.458	0.736	0.212	0.458	0.736
0.0035	0.463	0.333	0.752	0.463	0.752	0.212	0.463	0.752
0.0025	0.466	0.333	0.765	0.466	0.765	0.212	0.466	0.765
0.0015	0.467	0.333	0.773	0.467	0.773	0.212	0.467	0.773
0.0005	0.467	0.333	0.777	0.467	0.777	0.212	0.467	0.777

Table-3c : Various Coefficients of FGM2 (Nickel-Aluminum Oxide) Shell								
Z_m m	C_1 m^{-2} (10^4)	C_2 m^{-2} (10^5)	I_1 kgm^{-2} (10^2)	I_3 kg (10^{-2})	I_5 kgm^2 (10^{-6})	I_7 kgm^4 (10^{-10})	$-B_{31}$ (10^2)	$-C_{31}$ (10^{-2})
0.0095	0.333	0.100	0.672	0.240	0.152	0.113	0.841	0.761
0.0085	0.333	0.100	0.672	0.235	0.144	0.103	0.752	0.545
0.0075	0.333	0.100	0.672	0.230	0.138	0.097	0.664	0.375
0.0065	0.333	0.100	0.672	0.226	0.134	0.094	0.575	0.244
0.0055	0.333	0.100	0.672	0.223	0.131	0.093	0.487	0.148
0.0045	0.333	0.100	0.672	0.220	0.130	0.092	0.398	0.082
0.0035	0.333	0.100	0.672	0.218	0.129	0.092	0.310	0.039
0.0025	0.333	0.100	0.672	0.216	0.129	0.092	0.221	0.014
0.0015	0.333	0.100	0.672	0.215	0.129	0.092	0.133	0.003
0.0005	0.333	0.100	0.672	0.215	0.129	0.092	0.044	0.000

suppression time is observed when the magnetostrictive layers are placed farther away from the neutral plane. Similarly, from Figs. 4a-4d one can observe that, longest suppression time occurs when the magnetostrictive layer is located closest to the neutral plane of the shell.

Influence of the position of the magnetostrictive layers in the thickness direction from the neutral plane of the shell on the damping of the vibration response are listed in Tables-4 to 8. In Tables-4 to 7, the value of λ_0 increases when the magnetostrictive layer is located father away from the neutral axis, indicating faster vibration suppression. This is due to larger bending moment created by actuating force in the magnetostrictive layers. Further, it is observed that the damping parameter B_{31} and associated normalized value of B_n increases as the magnetostrictive layers are moved away from the neutral plane. These damping parameters are listed in Tables-2 and 3. These results qualitatively with the results presented in Pradhan et al. [16], He et al. [11] and Pradhan [17].

Table-4 : Suppression Time Ratio for Various Locations of Magnetostrictive Layers in FGM1 Shells h_m = 1*mm*

Z_m (m)	$-\lambda_0$	$\pm\omega_d$	W_{max} (mm)	t_s (S)	t_n
0.0095	9.760	778.57	1.259	0.244	0.055
0.0085	8.731	803.46	1.222	0.268	0.060
0.0075	7.702	828.79	1.184	0.305	0.068
0.0065	6.673	848.44	1.154	0.350	0.078
0.0055	5.645	862.38	1.113	0.410	0.092
0.0045	4.618	873.60	1.116	0.505	0.113
0.0035	3.591	886.54	1.097	0.647	0.145
0.0025	2.564	893.99	1.087	0.909	0.204
0.0015	1.612	892.53	1.091	1.501	0.336
0.0005	0.537	894.26	1.093	4.463	1.000

Table-5 : Suppression Time Ratio for Various Locations of Magnetostrictive Layers in FGM1 Shells h_m = 2*mm*

Z_m (m)	$-\lambda_0$	$\pm\omega_d$	W_{max} (mm)	t_s (S)	t_n
0.009	18.317	663.54	1.410	0.135	0.118
0.008	16.276	726.37	1.323	0.141	0.124
0.007	14.237	770.68	1.261	0.165	0.145
0.006	12.198	806.39	1.209	0.197	0.173
0.005	10.161	834.35	1.169	0.228	0.200
0.004	8.125	854.79	1.140	0.288	0.252
0.003	6.091	875.41	1.110	0.382	0.335
0.002	4.060	881.40	1.105	0.579	0.507
0.001	2.029	893.62	1.089	0.141	1.000

Effect of Thickness of Magnetostrictive Layers

Vibration response of FGM1 shell for various thicknesses of the magnetostrictive layers (hm) are studied. Magnetostrictive damping coefficients and natural frequencies for various thicknesses of magnetostrictive layers are listed in Tables-4 to 7. These damping coefficients and natural frequencie4s refer to the first mode of vibration. Vibration suppression time for hm equals to 1mm, 2mm, 3mm and 5m are listed in Tables-4, 5, 6 and 7 respectively. These computations are carried out for various locations (Z_m) of the magnetostrictive layers and listed

Table-6 : Suppression Time Ratio for Various Locations of Magnetostrictive Layers in FGM1 Shells h_m = 3*mm*

Z_m (m)	$-\lambda_0$	$\pm\omega_d$	W_{max} (mm)	t_s (S)	t_n
0.0085	25.702	562.13	1.636	0.092	0.179
0.0075	22.669	661.05	1.401	0.107	0.208
0.0065	19.637	723.98	1.318	0.124	0.241
0.0055	16.607	772.53	1.252	0.140	0.272
0.0045	13.578	812.17	1.196	0.172	0.334
0.0035	10.553	839.35	1.160	0.226	0.439
0.0025	7.533	858.58	1.135	0.309	0.600
0.0015	4.517	881.17	1.104	0.515	1.000

in Tables-4 to 7. The vibration suppression time (t_s) versus the distance of magnetostrictive layers from the neutral plane (Z_m) for various thicknesses of magnetostrictive layers (h_m) are plotted in Fig.5. This includes magnetostrictive layers of thicknesses (h_m) of 1mm, 2mm and 3mm at various locations. From Fig.5 one can observe that 1mm, 2mm and 3m at various locations. From Fig.5 one can observe that 1m thick magnetostrictive layer exhibits better attenuation as compared to 2mm and 3mm thick magnetostrictive layers.

Therefore, relatively thinner magnetostrictive layer leads to better attenuation characteristics. These results presented here agree qualitatively with the results presented in Pradhan et al. [16], He et al. [11] and Pradhan [17].

Effect of Vibration Modes

Effect of higher modes of vibration on the vibration suppression time is studied for the FGM1 shell. Transverse deflection versus time for various cases of the FGM shells are plotted in Figs.6-8. Figs.6a, 6b, 6c and 6d show the transient response of modes 1, 3, 5 and 7, respectively. It is observed that attenuation favours the higher modes. This is clearly seen in Figs. 7a and 7b, where modes 1 and 3 are compared for FGM1 and FGM2 shells. These figures indicate that mode 3 attenuates at a significantly faster rate as compared to mode 1. Present results in Figs.6a-6d also show that the vibration suppression time decreases very rapidly as vibration mode number increases. These vibration results for various modes agree qualitatively with the results presented in Pradhan et al. [16] and Pradhan [17].

Table-7 : Suppression Time Ratio for Two Different Control Gains and Various Locations of Magnetostrictive Layers in FGM1 Shells h_m = 5*mm*

	$C(t)\ r_c = 10^4$					$C(t)\ r_c = 10^3$				
Z_m (m)	$-\lambda_0$	$\pm\omega_d$	W_{max} (mm)	t_s (S)	t_n	$-\lambda_0$	$\pm\omega_d$	W_{max} (mm)	t_s (S)	t_n
0.0075	37.086	414.69	2.071	0.079	0.414	3.709	416.33	2.356	0.623	0.303
0.0065	32.119	565.15	1.594	0.081	0.424	3.212	566.06	1.735	0.724	0.383
0.0055	27.154	669.16	1.377	0.096	0.503	2,715	669.70	1.445	0.856	0.453
0.0045	22.188	743.32	1.282	0.104	0.545	2.219	743.65	1.334	1.024	0.542
0.0035	17.228	792.14	1.219	0.137	0.717	1.723	792.33	1.258	1.303	0.689
0.0025	12.279	831.79	1.168	0.191	1.000	1.228	831.88	1.194	1.890	1.000

Fig.4 Comparison of Uncontrolled (- - - - -) and Controlled (-----) Motion at the Midpoint of the FGM1 Shell for Various Locations of Magnetostrictive Layers, (a) Z_m = 3.5 m, (b) Z_m = 5.5 mm, (c) Z_m = 7.5 mm and (d) Z_m = 9.5 m

Effect of Intensity of Control Gain

Vibration suppression time (t_s) for the intensity of control gain $C(t)$ r_c values of 1,000 and 10,000 are computed and the results are listed in Table-7. This shows that increase of intensity of control gain results in proportional increase in vibration suppression time. From the results listed in Table-7, it is interesting to note that the suppression time ratio (t_s) is directly proportional to the control gain of the applied magnetic field.

Fig.5 Vibration Suppression Time t_s for Various Thicknesses of Magnetostrictive Layers (h_m)

Effect of Material Properties of FGM Shell

Effect of material properties of the FGM shell on the vibration suppression time is studied. Fig.8 displays the vibration suppression for FGM1 (Stainless Steel - Nickel) and FGM2 (Nickel - Aluminum Oxide) shells. For this comparison study Z_m is assumed to be 9.5mm. From Fig.8, it is observed that FGM1 shell has lower frequency compared to the FGM2 shell. This confirms that the FGM1 shell has lower flexural rigidity and thus a lower frequency compared to the FGM2 shell. These results agree qualita-

Table-8 : Vibration Suppression Using FSDT and HSDT

h/a	W_{max} (*FSDT*) (mm)	t_s (*FSDT*) (s)	W_{max} (*HSDT*) (mm)	t_s (*HSDT*) (s)
5	0.085	0.0395	0.129	0.0535
10	0.196	0.0294	0.258	0.0501
100	1.226	0.222	1.259	0.244

Fig.6 Vibration Suppression of Higher Modes at the Midpoint of the FGM1 Shell (a) n = 1, (b) n = 3, (c) n = 5 and (d) n = 7)

Fig.7 Comparison of Controlled Motion at the Midpoint of the (a) FGM1 and (b) FGM2 Shells for Vibration Modes n = 1 and n = 3

Fig.8 Vibration Suppression of FGM1 and FGM2 Shells for Z_m = 9.5 mm

tively with the results presented in Pradhan et al.[16] and Pradhan [17].

Effect of Higher Order Shear Deformation Theory

From Table-7, it is observed that employing HSDT the normalized suppression time ratio (t_n) is dependent on the intensity of control gain. While employing FSDT it is observed that the normalized suppression time ratio (t_n) is independent of the intensity of control gain. These results agree qualitatively with the results presented in Pradhan et al. [16] and Pradhan [17]. Normalized suppression time ratio (t_n) is dependent on the intensity of control gain reveals that HSDT takes into account the control gain in the analysis. Results are obtained for various *a/h* ratios and listed in Table-8. Here *h* and *a* represent the thickness of the shell and the arc length of the shell boundaries. From Rable-8 and Fig.9 one could observe that as the thickness of the shell decreases the maximum deflection increases for both FSDT and HSDT.

Fig.9 Vibration Suppression Using FSDT and HSDT for a/h Ratio (a) 100 and (b) 10

Further maximum deflections predicted by HSDT is larger than those from FSDT. For *a/h* ratio of 5 maximum deflection predicted by HSDT is 51 percent larger than

that of FSDT. While for *a/h* ratio of 100 maximum deflection predicted by HSDT is only 2 percent larger than that of FSDT. Further the suppression time (t_s) predicted by HSDT is larger than the corresponding results of FSDT. This is due to the fact that HSDT takes into account the shear forces along the thickness of the thick FGM shell. This study suggests that HSDT should be considered for the analysis of the thick FGM shell.

Conclusions

A theoretical formulation for a FGM shell with embedded magnetostrictive layers has been presented. The analytical solutions for the case of simply-supported boundary conditions has been derived, and numerical results are presented. The formulation is based on the higher order shear deformation shell theory (HSDT), and the analytical solution for the simply-supported shell is based on the Navier solution approach. The effects of the material properties of the FGM shell, thickness of magnetostrictive layers and location of the magnetostrictive layers on the vibration suppression time have been examined in detail. It was found that attenuation effects were better if the magnetostrictive layers were placed farther away from the neutral plane. Attenuation effects were also better when the magnetostrictive layers were relatively thinner. Further, suppression time ratio was directly proportional to the control gain of the applied magnetic field. Furthermore influence of higher order shear deformation shell theory is significant for the thick FGM shells.

Acknowledgement

Authors would like to acknowledge the technical discussions and suggestions of Professor J.N. Reddy, Texas A and M University, College Station, U.S.A.

References

1. Uchino, K., "Electrostrictive Actuators : Materials and Applications", Ceramics Bulletin, Vol.65, 1986, pp.647-652.

2. Cross, L.E. and Jang, S.J., "Electrostrictive Materials", Proceedings of "Recent Advances in Piezoelectric Ceramics. Electronic Ceramics, Properties, Devices and Applications", Marcel Dekker, Inc., New York, 1988, pp.129-137.

3. Crawley, E.F. and Luis, J.D., "Use of Piezoelectric Actuators and Elements of Intelligent Structure", AIAA Journal, Vol.25, 1987, pp.1373-1385.

4. Baz, A., Imam, K. and Mccoy, J., "The Dynamics of Helical Shape Memory Actuators", Journal of Intelligent Material Systems and Structures, Vol.1, 1990, pp.105-133.

5. Choi, Y., Sprecher, A.F. and Conrad, H., "Vibration Characteristics of a Composite Beam Containing Electrorheological Fluid", Journal of Intelligent Material Systems and Structures, Vol.1, 1990, pp.91-104.

6. Goodfriend, M.J. and Shoop, K.M., "Adaptive Characteristics of the Magnetostrictive Alloy, Terfenol-D, for Active Vibration Control", Journal of Intelligent Material Systems and Structures, Vol.3, 1992, pp.245-254.

7. Anjanappa, M. and Bi, J., "Magnetostrictive Mini Actuators for Smart Structural Application", Smart Materials and Structures, Vol.3 (4), 1994, pp.383-390.

8. Bryant, M.D., Fernandez, B. and Wang, N., "Active Vibration Control in Structures Using Magnetostrictive Terfenol with Feedback and/or Neural Network Controllers", Journal of Intelligent Material Systems and Structures, Vol.4, 1993, pp.484-489.

9. Krishna Murty, A.V., Anjanappa, M. and Wu, F.-F., "The Use of Magnetostrictive Particle Actuators for Vibration Attenuation of Flexible Beams", Journal of Sound and Vibration, Vol.206(2), 1997, pp.133-149.

10. Friedmann, PP., Carman, G.P. and Millott, T.A., "Magnetostrictively Actuated Control Flaps for Vibration Reduction in Helicopter Rotors Design Considerations for Implementation", Mathematical and Computer Modelling, Vol.33(10-11), 2001, pp.1203-1217.

11. He, X.Q., Liew, K.M., Ng, Y.Y. and Sivashankar, S., "A FEM Model for the Active Control of Curved FGM Shells Using Piezoelectric Sensor/Actuator Layers", International Journal of Numerical Methods in Engineering, Vol.54(6), 2002, pp.853-870.

12. Woo, J. and Meguid, S.A., "Nonlinear Analysis of Functionally Graded Plates and Shallow Shells", International Journal of Solids and Structures, Vol.38 (42-43), 2001, pp.7409-7421.

13. Pradhan, S.C., Loy, C.T., Lam, K.Y. and Reddy, J.N., "Vibration Characteristics of Functionally Graded Cylindrical Shells Under Various Boundary Conditions", Applied Acoustics, Vol.61(1), 2000, pp.111-129.

14. Loy, C.T., Lam, K.Y. and Reddy, J.N., "Vibration of Functionally Graded Cylindrical Shells", International Journal of Mechanical Science, Vol.41(3), 1999, pp.309-324.

15. Giurgiutiu, V., Jichi, F., Berman, J.B. and Kamphaus, J.M., "Theoretical and Experimental Investigation of Magnetostrictive Composite Beams", Smart Materials and Structures, Vol.10(5), 2001, pp.657-667.

16. Pradhan, S.C., Ng, T.Y., Lam, K.Y. Reddy, J.N., "Control of Laminated Composite Plates Using Magnetostrictive Layers", Smart Materials and Structures, Vol.10(4), 2001, pp.657-667.

17. Pradhan, S.C., "Vibration Suppression of FGM Composite Shells Using Embedded Magnetostrictive Layers", International Journal of Solids and Structures, Vol.42(9-10), 2005, pp.2465-2488.

18. Reddy, J.N., "A Refined Nonlinear Theory of Plates with Transverse Shear Deformation", International Journal of Solids and Structures, Vol.20(9-10), 1984, pp.881-893.

19. Reddy, J.N., "Exact Solutions of Moderately Thick Laminated Shells", Journal of Engineering Mechanics, ASCE, Vol.110(5), 1984, pp.794-809.

20. Reddy, J.N., "Mechanics of Laminated Composite Plates, Theory and Analysis", Boca Raton, FL : Chemical Rubber Company, 1997.

21. Reddy, J.N. and Liu, C.F., "A Refined Shear Deformation Theory of Laminated Shells", International Journal of Engineering Science, Vol.23(3), 1985, pp.319-330.

Appendix

$$S_{11} = A_{11}\alpha^2 + A_{66}\beta^2$$

$$S_{12} = A_{12}\alpha\beta + A_{66}\alpha\beta$$

$$S_{13} = -A_{11}\frac{1}{R_1}\alpha - A_{12}\frac{1}{R_2}\alpha - C_1 E_{11}\alpha^3 - C_1 E_{12}\alpha\beta^2 - C_1 E_{66}2\alpha\beta^2$$

$$S_{14} = B_{11}\alpha^2 - C_1 E_{11}\alpha^2 + B_{66}\beta^2 - C_1 E_{66}\beta^2$$

$$S_{15} = B_{12}\alpha\beta - C_1 E_{12}\alpha\beta + B_{66}\alpha\beta - C_1 E_{66}\alpha\beta$$

$$S_{21} = S_{12}$$

$$S_{22} = A_{66}\alpha^2 + A_{22}\beta^2$$

$$S_{23} = -2C_1 E_{66}\alpha^2\beta - A_{12}\frac{1}{R_1}\beta - A_{22}\frac{1}{R_2}\beta - C_1 E_{12}\alpha^2\beta - C_1 E_{22}\beta^3$$

$$S_{24} = B_{66}\alpha\beta - C_1 E_{66}\alpha\beta + B_{12}\alpha\beta - C_1 E_{12}\alpha\beta$$

$$S_{25} = B_{66}\alpha^2 - C_1 E_{66}\alpha^2 + B_{22}\beta^2 - C_1 E_{22}\beta^2$$

$$S_{31} = S_{13}$$

$$S_{32} = S_{23}$$

$$S_{33} = A_{55}\alpha^2 - 2C_2 D_{55}\alpha^2 + A_{44}\beta^2 - 2C_2 D_{44}\beta^2 + C_2^2 F_{55}\alpha^2$$
$$+ C_2^2 F_{44}\beta^2 + 2C_1 E_{11}\frac{1}{R_1}\alpha^2 + 2C_1 E_{12}\frac{1}{R_2}\alpha^2 + C_1^2 H_{11}\alpha^4 + C_1^2 H_{12}\alpha^2\beta^2$$
$$+ 2C_1^2 H_{66}\alpha^2\beta^2 + 2C_1 E_{12}\frac{1}{R_1}\beta^2 + 2C_1 E_{22}\frac{1}{R_2}\beta^2 + C_1^2 H_{12}\alpha^2\beta^2 + C_1^2 H_{22}\beta^4$$
$$- A_{11}\frac{1}{R_1^2} - 2\frac{1}{R_1 R_2}A_{12} - A_{22}\frac{1}{R_2^2}$$

$$S_{34} = A_{55}\alpha - 2C_2 D_{55}\alpha + C_2^2 F_{55}\alpha - C_1 F_{11}\alpha^3 + C_1^2 H_{11}\alpha^3$$
$$- 2C_1 F_{66}\alpha\beta^2 + 2C_1^2 H_{66}\alpha\beta^2 + C_1^2 H_{12}\alpha\beta^2 - \frac{1}{R_1}B_{11}\alpha$$
$$+ C_1\frac{1}{R_1}E_{11}\alpha - \frac{1}{R_2}B_{12}\alpha + C_1\frac{1}{R_2}E_{12}\alpha$$

$$S_{35} = A_{44}\beta - 2C_2 D_{44}\beta + C_2^2 F_{44}\beta - C_1 F_{12}\alpha^2\beta + C_1^2 H_{12}\alpha^2\beta$$
$$- 2C_1 F_{66}\alpha^2\beta + 2C_1^2 H_{66}\alpha^2\beta - C_1^2 F_{22}\beta^3 + C_1^2 H_{22}\beta^3$$
$$- \frac{1}{R_1}B_{12}\beta + C_1\frac{1}{R_1}E_{12}\beta - \frac{1}{R_2}B_{22}\beta + C_1\frac{1}{R_2}E_{22}\beta$$

$$S_{41} = S_{14}$$

$$S_{42} = S_{24}$$

$$S_{43} = S_{34}$$

$$S_{44} = D_{11}\alpha^2 - 2C_1F_{11}\alpha^2 + D_{66}\beta^2 - 2C_1F_{66}\beta^2 - A_{55} + 2C_2D_{55} - C_2^2F_{55} + C_1^2H_{11}\alpha^2 + C_1^2H_{66}\beta^2$$

$$S_{45} = D_{66}\alpha\beta + D_{12}\alpha\beta - 2C_1F_{66}\alpha\beta - 2C_1F_{12}\alpha\beta + C_1^2H_{12}\alpha\beta - C_1F_{66}\alpha\beta + C_1^2H_{66}\alpha\beta$$

$$S_{51} = S_{15}$$

$$S_{52} = S_{25}$$

$$S_{53} = S_{35}$$

$$S_{54} = S_{45}$$

$$S_{55} = D_{66}\alpha^2 - 2C_1F_{66}\alpha^2 + D_{22}\beta^2 - 2C_1F_{22}\beta^2 - A_{44} + 2C_2D_{44} - C_2^2F_{44} + C_1^2H_{66}\alpha^2 + C_1^2H_{22}\beta^2 \quad (49)$$

$$C_{13} = A_{31}\alpha$$

$$C_{23} = A_{32}\beta$$

$$C_{33} = -C_{31}\alpha^2 - C_{32}\beta^2 + \frac{A_{31}}{R_1} + \frac{A_{32}}{R_2}$$

$$C_{43} = B_{31}\alpha - C_1C_{31}\alpha$$

$$C_{53} = B_{32}\beta - C_1C_{32}\beta \quad (50)$$

$$M_{11} = \bar{I}_1$$

$$M_{12} = 0$$

$$M_{13} = \bar{I}_3\alpha$$

$$M_{14} = \bar{I}_2$$

$$M_{15} = 0$$

$$M_{21} = 0$$

$$M_{22} = \bar{J}_1$$

$$M_{23} = \bar{J}_3\beta$$

$$M_{24} = 0$$

$$M_{25} = \bar{J}_2$$

$$M_{31} = M_{13}$$

$$M_{32} = M_{23}$$

$$M_{33} = \bar{I}_1 + C_1^2I_7(\alpha^2 + \beta^2)$$

$$M_{34} = \bar{I}_5\alpha$$

$$M_{35} = \bar{J}_5\beta$$

$$M_{41} = M_{14}$$

$$M_{42} = 0$$

$$M_{43} = M_{34}$$

$$M_{44} = \bar{I}_4$$

$$M_{45} = 0$$

$$M_{51} = 0$$

$$M_{52} = M_{25}$$

$$M_{53} = M_{35}$$

$$M_{54} = 0$$

$$M_{55} = \bar{J}_4 \quad (51)$$

where the magnetostrictive coefficients $A_{31}, A_{32}, B_{31}, B_{32}, C_{31}$ and C_{32} are defined in equation (27).